11. MEDITERRANEAN RIDGE, LEVANTINE SEA – SITE 130

The Shipboard Scientific Party[1]

SITE DATA

Occupied: September 16-18, 1970.

Position: In the region of elongate ridges and troughs on the Mediterranean Ridge, north of the Herodotus Abyssal Plain.
Latitude: 33° 36.31′N;
Longitude: 27° 51.99′E.

Holes Drilled: Two holes (130 and 130A).

Water Depth: 2979 and 2982 meters, respectively.

Cores Taken: Seven and one, respectively.

Total Penetration: 563 and 11 meters, respectively.

Deepest Unit Recovered: Detrital sandstones of Quaternary age.

MAIN RESULTS

Two holes were drilled at Site 130. The first penetrated a thick sequence of terrigenous muds, sands, and sandstones more than 500 meters in thickness, sparsely intercalated with pelagic marl oozes of Quaternary age. Sedimentary textures and primary bedding structures suggest that the terrigenous layers of this formation were deposited for the most part by turbidity currents, and mineralogical investigations of both the fine- and coarse-grained detrital components suggest a North African (Nile River) provenance.

The second hole included a core punched directly into the upper sea bed and established that the contemporary ridge surface at the site is blanketed by a layer of pelagic sediment 14.5 meters in thickness.

It is concluded that the southern flank of the Mediterranean Ridge here is an uplifted and deformed wedge of basinal sediments, previously deposited on a once extensive abyssal plain seaward of the Nile Cone. Assemblages of foraminifera and dated sequences of sapropelitic mud and volcanic tephra in the superficial layer of pelagic sediment indicate that uplift of the sea bed isolated this part of the ridge from terrigenous deposition of Nile origin sometime around a half million years ago.

BACKGROUND

A resolution to encourage the drilling of a deep hole into the Mediterranean Ridge north of the Nile Cone can be traced by members of the Mediterranean Advisory Panel to the summer of 1964. At that time the R/V *Chain* of the Woods Hole Oceanographic Institution was pioneering the first continuous seismic-refraction traverse of the Levantine Basin of the eastern Mediterranean. The freshly obtained records of the subbottom layering showed an apparent continuation of acoustically stratified and horizontally layered sediments of the lower Nile Cone and Herodotus Abyssal Plain out onto the southern flank of the Mediterranean Ridge, where they were discovered to be tilted and folded.

This extension of sediment layers inferred to be of terrigenous origin onto a topographic high was considered highly unusual. In an invited paper at the 17th Symposium of the Colston Research Society (1965), J. B. Hersey, who had been Chief Scientist of the *Chain* expedition, reported that his own research and that of his students had indicated that acoustically stratified sediment bodies were generally confined to topographic depressions (i.e. basins or sediment ponds) which contain interstratified layers of sand, silt and clay brought in by turbidity currents. Since it was generally held that turbidity currents were incapable of travelling uphill, it was reasoned that the anomalous presence of stratified sediment on the Mediterranean Ridge must be a manifestation of some youthful uplift of a part of a previously more extensive abyssal plain.

The folding and faulting of sediment bodies in the ridge revealed in the seismic profiles (e.g., see Plate 16 of Hersey, 1965) were linked to deforming processes that resulted in the creation of many small blocks of fractured material. "Where rocks so fractured are overlain by sediments a comparable disturbance can be transmitted to the latter, particularly if they have developed some rigidity. In such a manner, the cobblestone areas might have been formed." (Hersey, 1965, p. 87). The details of this process became a major stimulus to the eventual drilling of DSDP Site 130, which this chapter reports.

The Basic Structure of the Ridge

Since the recognition of a broad central topographic swell in the eastern Mediterranean in the early precision echograms of *Vema, Atlantis*, and *Chain*, in the late 1950's and then its lateral delineation in the bathymetric charts of Goncharov and Mikhaylov (1963), Mikhaylov (1965), Emery *et al.* (1966), and Giermann (1966, 1968), there has been the nagging question as to its structure and origin.

Refraction Results

The first seismic refraction measurements obtained during the around-the-world cruise of HMS *Challenger* in 1952 substantiated at two stations in the Ionian Sea and one in the Levantine Sea south of Cyprus that the superficial unconsolidated layer of sedimentary materials ($V_p \leq 2.1$ km/sec) is generally thin (only 0.3-0.4 km thick), and that it overlies a refracting interface of significantly

[1]W. B. F. Ryan, Lamont-Doherty Geological Observatory; K. J. Hsü Eidg. Technische Hochschule; M. B. Cita, Universita degli Studi di Milano; Paulian Dumitrica, Geological Institute, Bucharest; Jennifer Lort, University of Cambridge; Wolf Maync, Geological Consulting Service, Berne, Switzerland; W. D. Nesteroff, Université de Paris; Guy Pautot, Centre Oceanologique de Bretagne; Herbert Stradner, Geologische Bundesanstalt, Vienna; F. C. Wezel, Universita di Catania.

higher compressional wave velocity (4.3-4.7 km/sec). This interface has subsequently been shown by reflection profiling (Hersey, 1965; Watson and Johnson, 1969; Wong and Zarudzki, 1970; and Ryan *et al.*, 1971) to be extensive throughout the eastern Mediterranean; it corresponds to what is referred to in this volume as Reflector M and was established by the *Glomar Challenger* drill holes to be the top of an evaporite layer of late Miocene age.

Along the southern flank of the Mediterranean Ridge, directly seaward of the Herodotus Abyssal Plain, the reflection data have revealed a significantly greater thickness of sediment above Reflector M than elsewhere on the ridge (see isopachs of Wong and Zarudzki, 1969, and Plate 16 of Hersey, 1965). The thickening of the sedimentary layer collaborated in refraction and deep reflection profiles of Moskalenko (1966) (Figure 1) and in surface-wave dispersion curves presented by Payo (1967) has been the focus of recent scientific inquiry.

In discussions of possible origins of the ridge, Emery *et al.* (1966) noted that the region of thicker sediment is characterized by coarse-textured surface relief (hills of 100- to 300-meter amplitude) caused by some process of sedimentary deformation.

Cause of the Sediment Thickening and Deformation

Most researchers have related the northward increase in the crustal thickness of the eastern Mediterranean to processes accompanying the subduction of lithosphere beneath the Hellenic Arc (McKenzie, 1970, Caputo *et al.*, 1970; Papazachos and Comninakis, 1971; Wong *et al.*, 1971. Using profiles of free air and Bouguer corrected gravity anomalies, Woodside and Bowin (1970) and Rabinowitz and Ryan (1970) were able to show in simplified structural sections that a significant northward dip of the Moho (up to 7 degrees) exists at the southern boundary of the Mediterranean Ridge. However, differences of opinion exist as to the cause of the crustal thickening that has apparently accompanied the downward flexure of the crustal layers.

For instance, Woodside and Bowin (1970) suggest that the extra crustal material is comprised of a "contingent thick accumulation of sediment in the depression formed south of the European overthrust block" (p. 1119). They infer that these sediments were "rapidly supplied to the marginal trough just south of the thrust sheet from the elevated crustal material of the overthrusting mass" (p. 1120). This hypothesis implies post- or syntectonic sedimentation of northern (internal) provenance.

Other researchers, also basing their interpretations on gravity data, have linked the thickening mechanism to tectonic superposition of previously deposited sedimentary materials of originally southern (external) provenance. In the schemes portrayed in structural models of Dewey and Bird (1970) and Ryan and Rabinowitz (1970), the Mediterranean Ridge marks a zone of crustal shortening involving slices of sediment (flysch?) deposited prior to downflexure of the African lithospheric plate.

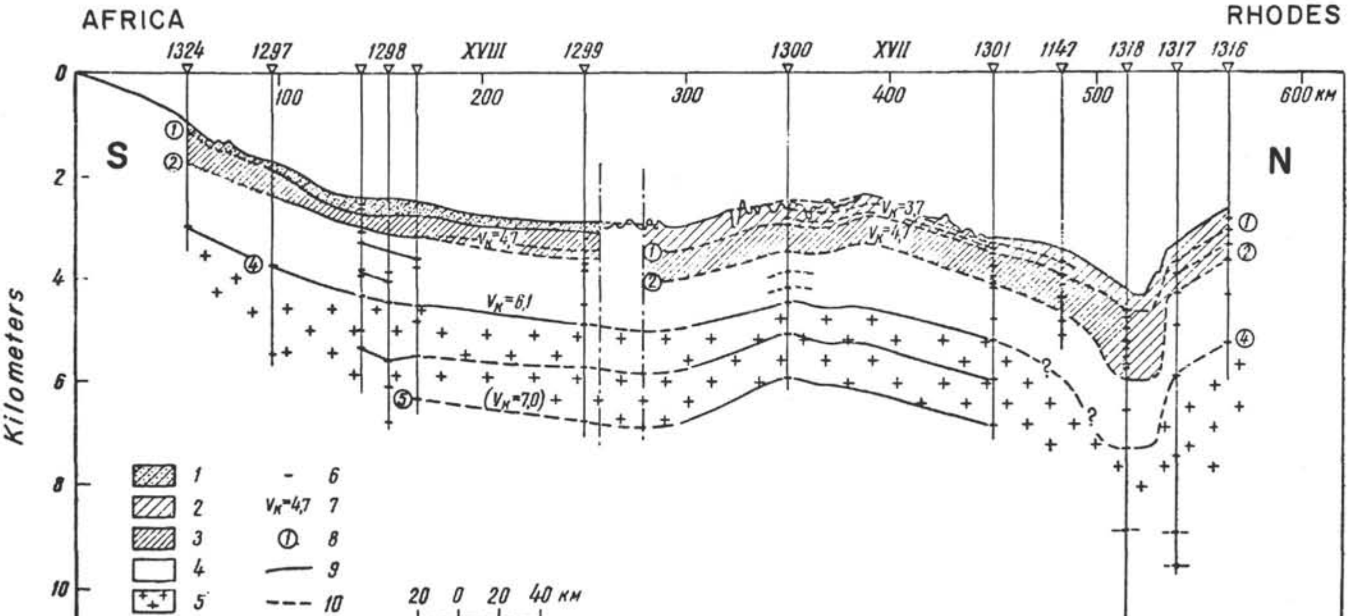

Figure 1. *Interpretation of a structure section across the eastern Mediterranean from Egypt to Rhodes based on refraction and deep point-reflection data (after Moskalenko, 1966). (1) Unconsolidated sediments in the North African continental margin; (2) Unconsolidated sediments on the basin floor; (3) semiconsolidated sediments; (4) consolidated sediments; (5) basement; (6) reflecting horizon; (7) compressional-wave velocity in km/sec for refracted arrivals from the upper surface of the subjacent layer; (8) interpretation of the interfaces of major crustal layers; (9) a confident correlation; (10) an interpretive or speculative correlation; (11) zone in which correlations are absent. Note the much greater thickness of unconsolidated sediment on the Mediterranean Ridge at Station 1300.*

Objectives of Drilling

The question of whether the sediment comprised in the stratified layering of the Mediterranean Ridge has come from the south or the north was considered directly answerable by deep subbottom sampling. Considerable data had been already gleaned from Neogene sequences of North Africa (bore holes and outcrops) so as to allow one to quite precisely delineate if offshore submarine deposits possessed a Nile River or Sahara Desert provenance (see, for instance Elgabaly and Khadar, 1962; Chumakov, 1967; Sukhri, 1950 and 1951; and Butzer and Hansen, 1965).

Conversely, the metamorphic terranes and limestone platforms of Greece and Turkey are characterized by diagnostic mineral and fossil assemblages foreign to the African margin (Emelyanov, 1968; Venkatarathnam and Ryan, 1971; Venkatarathnam *et al.*, 1971; Van der Kaaden, 1971; and Bremer, 1971).

Therefore, the Mediterranean Advisory Panel considered it a rather straightforward primary objective to drill a carefully selected hole in the region of coarse-textured relief to test the above mentioned hypotheses as to the source of the thick sediments in the Ridge. Furthermore, since all the models had suggested uplift of a stratified basinal type of sediment, irrespective of its provenance or petrological composition, the panel reasoned that carefully spaced coring intervals might locate a level where predominantly grainflow and turbidity-current deposits would be superseded by carbonate-rich oozes of pelagic origin allowing a date to be placed on the commencement of the uplift and consequent isolation of the ridge surface from continental detritus.

Site Selection

A strategically placed south to north transit of the lower Nile Cone and Mediterranean Ridge was obtained in 1965 by the R/V *Robert D. Conrad* under the scientific direction of M. Ewing of the Lamont-Doherty Geological Observatory. Along this track through the area of coarse-textured relief, it is possible to trace on the reflection profiles individual subbottom reflecting horizons of the Cone directly onto the southermost hills of the ridge as illustrated in Figure 2. These hills (particularly along the southern end of the profile) have the appearance of very gentle folds. Where the folds become steeper, toward the north, internal reflections disappear, and it is no longer possible to delineate subbottom layering. However, based on a small detailed grid survey of a few of the anticlinal features by the *Robert D. Conrad*, where underway tracks are parallel to the topographic grain, internal stratification often can be detected. Since the stratification appears both on the crests of topographic highs as well as in the lows, it is likely that material of similar acoustic reflectivity is present throughout the region of coarse-grained textures and is masked primarily by geometric (i.e. ray path focusing and scattering) factors.

A single piston core (RC9-178) from near the crest of one of the highs recovered a dark gray, carbonate-poor, fine-grained terrigenous mud with scattered nannofossils of Upper Pliocene age (see Figure 19 of Ryan *et al.*, 1971). This single lithologic unit found a few centimeters above the base of the core at an angular unconformity below carbonate-rich pelagic oozes of Late Pleistocene age was an initial clue that terrigenous clastics were present in the

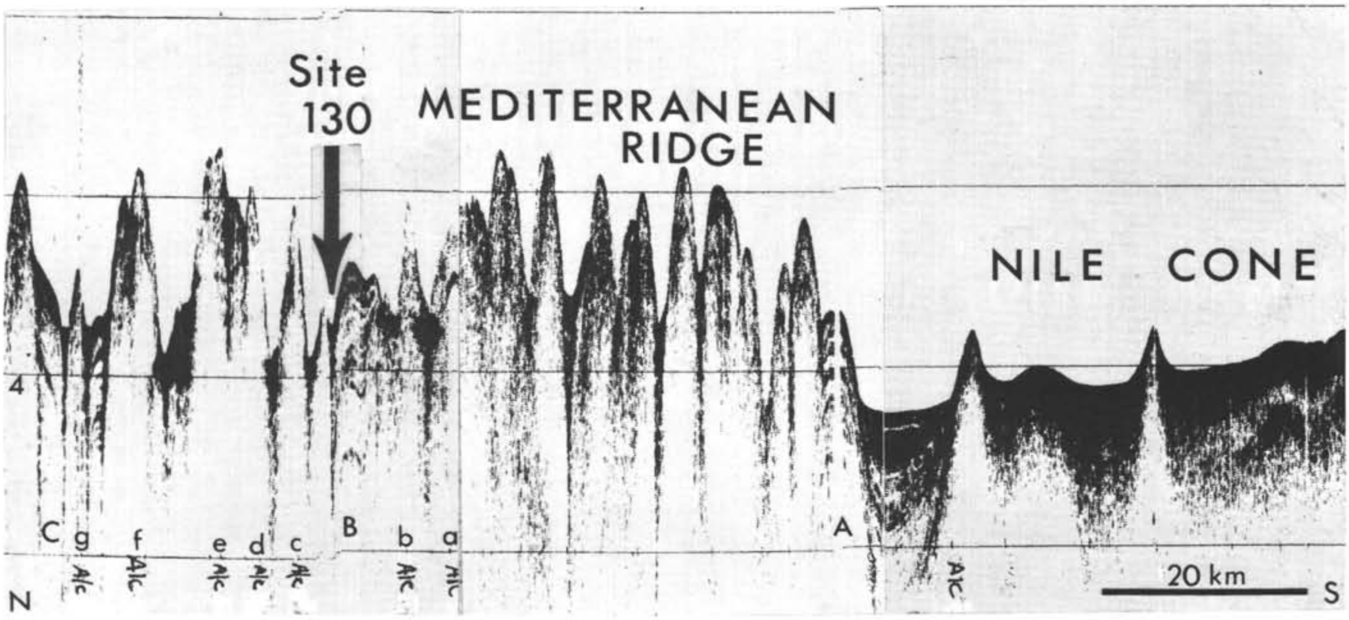

Figure 2. *North-south seismic reflection profile across the Mediterranean Ridge and Nile Cone made by the* Robert D. Conrad *in 1965 using an airgun sound source. Observe the stratified layering beneath the lower cone which can be traced up onto the first hill of the southern flank of the Ridge (A). Stratification reappears in a survey area near Drillsite 130 along tracks parallel to the topographic grain (B and C). Vertical scale is in two-way reflection time (seconds). A/C's indicate course changes and the lower case letters show these positions on the survey plan of Figure 5.*

subsurface layers of the ridge, but the sample obtained was too small and restricted to permit any sweeping conclusions as to its provenance or origin.

Other Considerations

Although it was agreed upon to place the *Glomar Challenger* drill hole close to the site of this piston core, a consulting panel to the Deep Sea Drilling Project warned that drilling on the crest of one of the folds might involve the risk of penetrating a hydrocarbon reservoir. Since this opinion was certainly justifiable in light of the significant organic carbon content of the RC9-178 Pliocene sample, an alternate site was chosen away from the crest of a fold structure at a site about 10 kilometers to the south of the location of the piston core. The new site presented far less of a pollution risk, and showed some subsurface stratification which would allow a geophysical correlation to the drilled sedimentary section.

Strategy

Satellite navigation had been employed during the *Conrad* survey so that the prospective target could be accurately pinpointed. After completing Site 129 in the Strabo Trench, it was decided to proceed directly to the Mediterranean Ridge site without the necessity of conducting additional surveys. The profiling gear was streamed along with the magnetometer, so that if during the course of approach to the selected location a more optimum configuration of subbottom stratification was revealed, the drilling vessel could relocate on its own track.

***Challenger* Site Approach**

The departure from Site 129 took the *Glomar Challenger* first across the region of fine-textured relief on the Mediterranean Ridge. Proceeding southeast on a course of 140 degrees, Reflector M was seen at 0530 hours on September 16th on the reflection profile (Figure 3) beginning its descent beneath ever greater thicknesses of sediment concurrent with a gradual increase in sea floor relief (Figure 4).

At 074 hours the drilling vessel received a satellite fix which placed her projected intersection with the *Robert D. Conrad* survey area to the north of the target location. Corrective action was taken at 0821 hours with a course change to 166 degrees (Figure 5). By this time some stratification became apparent in the subsurface, and we were able to estimate the sediment thickness above Reflector M as probably greater than 2 seconds (two-way travel time). However, with no satellite pass scheduled during the next 2 hours of steaming before arrival, a decision was made to dead reckon directly to the drilling target and drop a buoy at the first optimum location on the underway seismic reflection profile. Unfortunately, however, the profiler resolution became increasingly poor in the

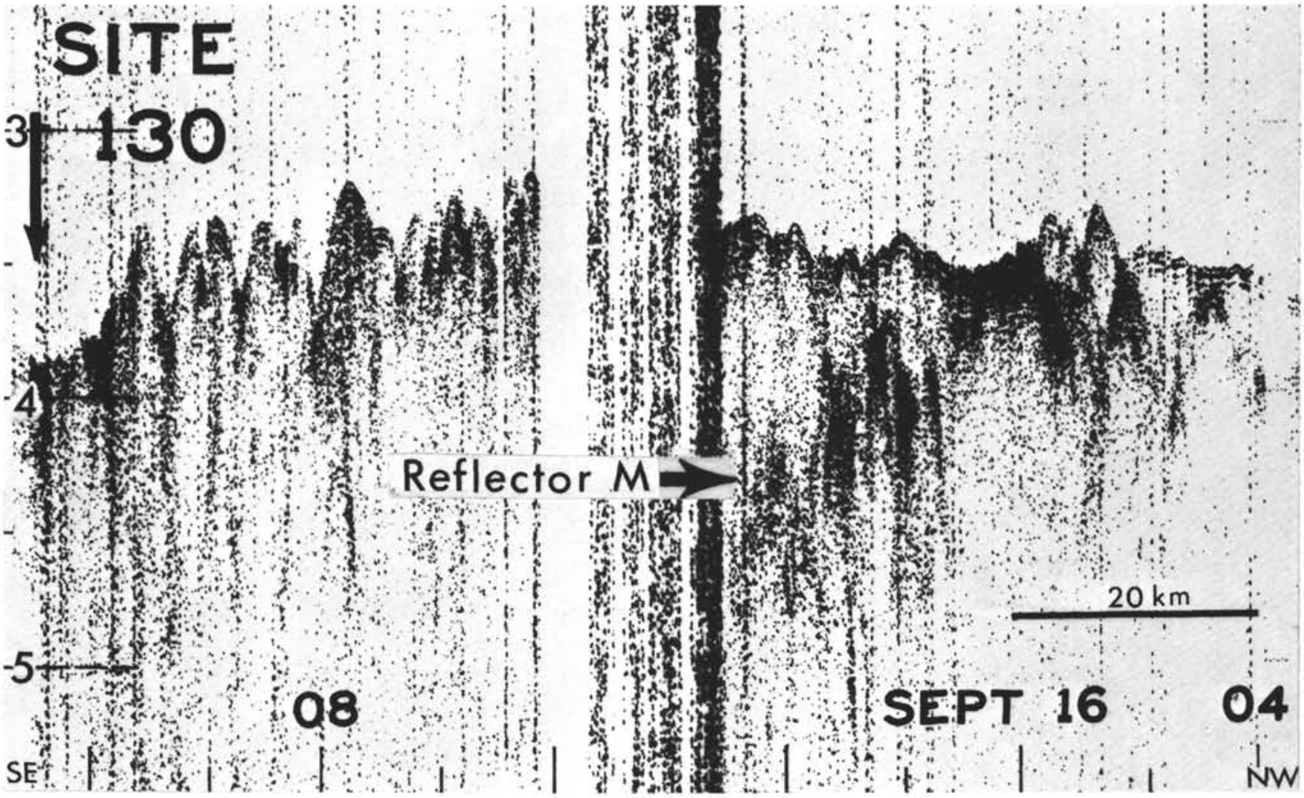

Figure 3. *Seismic reflection profile of the* Glomar Challenger *showing a crossing of the Mediterranean Ridge while proceeding to Site 130. Note the descent of Reflector M towards the southeast and an increase in the amplitude and wave length of the surface relief. Vertical scale is in two-way reflection time (seconds). Vertical exaggeration is* $\approx 28:1$.

region of coarse-textured relief and subbottom definition deteriorated.

At 0912 hours we recognized a low depression on the 12 kHz echogram very similar to a charted feature in the target area. Believing that a satisfactory location for the drilling objectives under consideration had been reached, a free-floating marker buoy was ejected while the ship maintained course and slowed to 4 kt to pull in the seismic gear and magnetometer. At 0926 hours with the gear secured, the ship reversed course to 310 degrees.

By the time the gear was secured at 0926 hours the vessel had set to the south beyond the topographic depression. Turning first to the east and then soon northward, the fathometer began to show a descent back downslope. At 0945 hours, finding a smooth stratified sea bed at 1540 tau water depth, the acoustic positioning beacon was emplaced – this time accompanied by a new experimental release mechanism so that we could call it back after completion of the drill hole.

Subsequent satellite fixes obtained during the next two days while completing the hole, placed the actual drilling site about one kilometer southwest of the original target on what turned out to be the southern flank of a broad, low linear hill adjacent to a small, flat sediment pond, an ideal location for a good pelagic blanket with possible displaced sediment from the neighboring hills. The water depth was determined from the fathogram to be 2943 meters (corrected for sound-velocity), and the hole was spudded into at 2989 meters from the derrick platform by drill string measurements.

OPERATIONS

The *Glomar Challenger* stayed on site from 0945 hours September 16th to 0710 hours September 18th. Not wishing to spend an excess amount of time continously coring from the sea bed down to the first encounter with the expected terrigenous strata, the shipboard scientific party decided to spot core at ever increasing intervals, and then later on drill a second offset hole to poinpoint the facies contact. The core inventory of Site 130 is given in Table 1.

The initial bottom contact at 2989 meters from the rig floor was quite uncertain; in fact some of those on the rig floor at that time thought they saw a slight rise in circulation pressure at 2969 meters. In washing down, a firm layer was abruptly encountered at only 3 meters below bottom. Penetration became difficult without rotation, until at 9 meters the bit broke through this hard zone and went back into washable, but firm sediment. Core 1 was cut from 13 to 23 meters upon completion of the next pipe section. It became necessary to apply slight circulation and some slow rotation to prevent jamming. When the core came up, everyone was suprised to see that we had already encountered and recovered the terrigenous mud facies, – a dark, blue black, carbonate-poor, plastic, sticky lithology. A decision was made to press on to a considerably greater subbottom depth and explore the stratigraphy of this deposit.

Core 2 was cut from 49 to 58 meters below bottom, and Core 3 from 77 to 86 meters. Penetration between the cored intervals was accomplished by washing under high circulation with the core barrel seated in the bit.

Cores 4 and 5 proceeded with very smooth and relatively easy drilling (Figure 6). A single thin interval of extremely firm material was encountered at 369 to 373 meters, and the drilling rate slowed significantly, only to rise again after a few more meters of penetration.

The cutting of Core 6 was initiated at 411 meters; after only a few meters of easy going we found ourselves in another stiff formation. In fact, fifty minutes were required to cut the last 5 meters of this core. Thus for the next stretch of the section it was decided to drill ahead with a center bit in place, instead of an empty core barrel.

Two notably hard horizons were encountered at 454 meters and 554 meters. Core 7 was cut into the latter which proved to be an extremely coarse-grained conglomerate sandstone.

Hole 130 was then terminated at 563 meters. Since ship time was urgently needed to explore the remaining scientific objective of learning the age of the top of the terrigenous sequence, not to mention additional high priority objectives at several sites yet to be drilled, we decided reluctantly to refrain from deeper penetration here. The string was pulled out and the hole cemented.

Offset Hole 130A

Hole 130A included only one surface core which was needed to sample the topmost section that had been missed in the original hole. This second hole was offset 100 feet south from the original hole. Coring was first attempted at 2968 to 2981 meters and then at 2981 to 2992 meters below the rig floor, only to embarrassingly come up with water and the absence of a mud smear on the core catchers. A sediment core was finally retrieved on the third attempt, after bottom contact was definitely confirmed at 2992 meters. This core contained 1.5 meters of pure pelagic sediment of Late Quaternary age similar in facies to the sediment found in the top of Core 1 of Hole 130.

With the second objective of establishing the presence of a superficial blanket of material without terrigenous intercalations now satisfactorily completed, the offset hole was abandoned after successfully testing the beacon release mechanism and retrieving the first electronic positioning package from the sea bed in the more than two year history of the Deep Sea Drilling Project.

A Reed PD-2 bit was used which again proved a most effective tool to drill through marly and shaly sediments. However, the core recovery, especially that of sandy sections, was extremely poor. It now seems clear to us that this type of bit should only be used if a rapid deep penetration through stiff marls is desired, and if continuous coring is not part of the main objectives.

BIOSTRATIGRAPHY

All eight cores recovered at Site 130 on the Mediterranean Ridge are believed to be Quaternary in age, although it may be possible that Cores 6 and 7 are as old as latest Pliocene.

Purely pelagic sediments without terrigenous intercalations were found only in the 130A core cut from the surface of the sea bed. In all other cores recovered from this

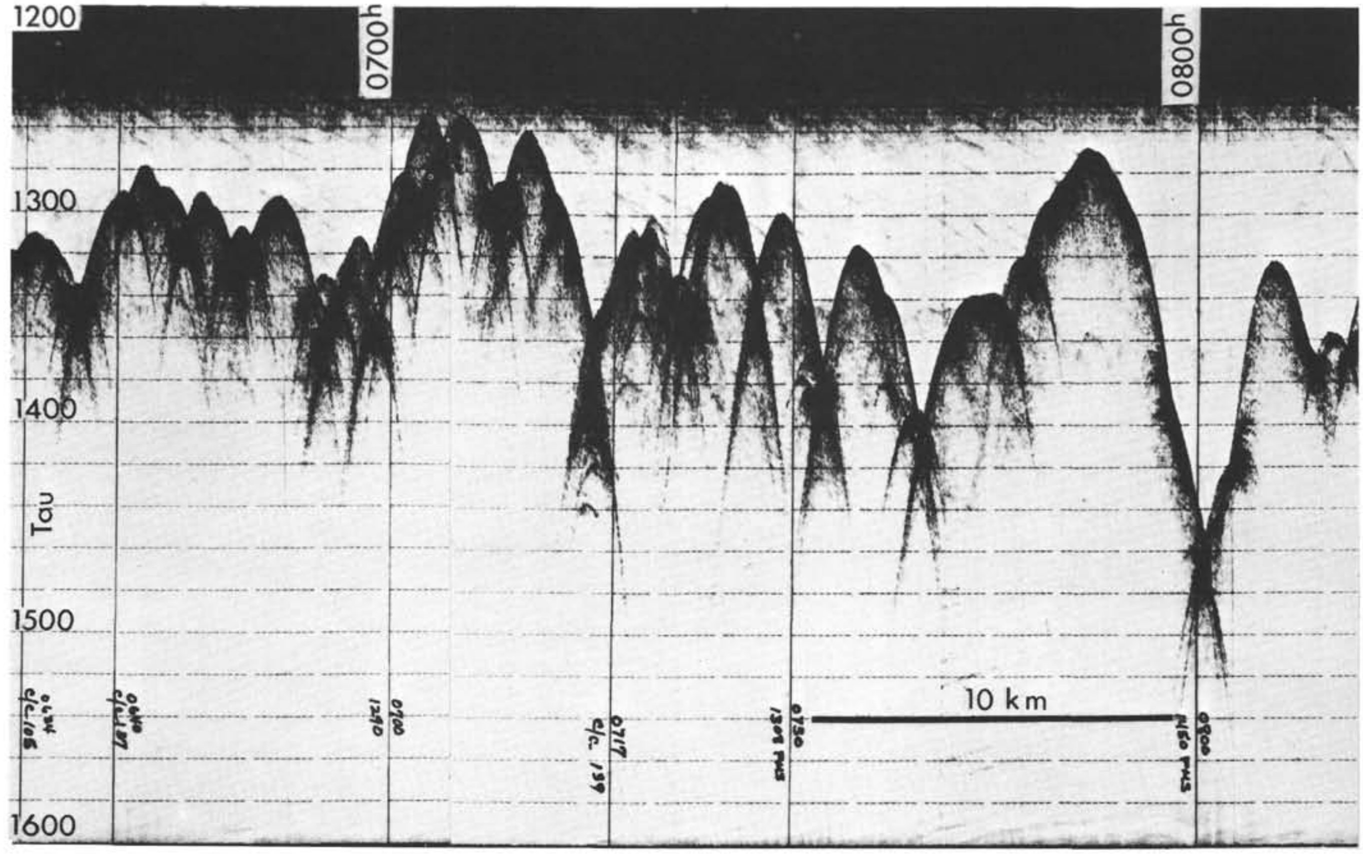

Figure 4. *Echo-gram of the Mediterranean Ridge traverse during the* Glomar Challenger *site approach. The amplitude of the so-called "cobblestone" relief (Hersey, 1965 and Emery* et al., *1966) progressively increases towards the south. Site 130 was located in a regionally smooth, low-lying area where sub-bottom stratification could be observed in reflection profiles.*

site the sediments are the results of the interaction of pelagic, mostly biogenic deposition, and terrigenous deposition, mainly in the form of fine-grained (primarily mud) turbidites.

The best represented fossil groups are foraminifera and calcareous nannoplankton. Also present are pteropods, fragments of pelecypods, otoliths, holothurian sclerites, hystricospherids, micrascidites of tunicates, spores, siliceous sponge spicules, and Radiolaria. The last are common to abundant at different levels of Core 6. Organic matter is also commonly present, especially in the terrigenous, or sapropel layers.

A layer of distinctly winnowed fossil remains including a large amount of pteropods, thin shelled pelecypods, and foraminifera indicating warm water, eutrophic conditions, and including displaced shallow water benthoic forms, is present in Core 130-3-2, 23-25 cm.

Reworked Cretaceous (*Globotruncana* sp.) and Pliocene (*Globigerinoides obliquus extremus*) planktonic foraminifera were noted in the center bit sample between Cores 6 and 7 and in the core catcher sample of Core 7.

Paleoenvironment and Rates of Sedimentation (M.B.C.)

A detailed investigation was carried out on the only section recovered from Core 1, Site 130A, in order to relate the faunal assemblages found there to climatic fluctuations in the younger parts of the Quaternary. Only the topmost core of the Mediterranean Ridge was chosen because this was the only satisfactory interval, where the faunal composition had not been affected by physical processes accompanying the periodic influx and intercalation of terrigenous layers (i.e. erosion or winnowing, etc.).

Twelve Core 1 samples were examined, averaging one every 12.5 centimeters. The distribution of thirty species of foraminifera in these samples is given in Table 2. An interpretation of assemblages in terms of an inferred climatic curve, faunal diversity, and total faunal abundance appears in Columns 1, 2, and 3 of Figure 7. The following comments concern the climatic implications of these samples.

The indications of cold, cold-temperate, temperate-cold, temperate, temperate-warm, warm-temperate climates, respectively, are based exclusively on the visual estimates of the relative abundance of the following species:

Globigerina pachyderma *Globigerina bulloides* *Globorotalia scitula*	cold water indicators
Globorotalia inflata	temperate water indicator
Hastigerina siphonifera *Hastigernina pelagica* *Globigerinoides conglobatus* *Globigerinoides ruber* *Globigerinoides sacculifer* *Globigerina digitata* *Globorotalia truncatulinoides* *Orbulina universa*	warm water indicators

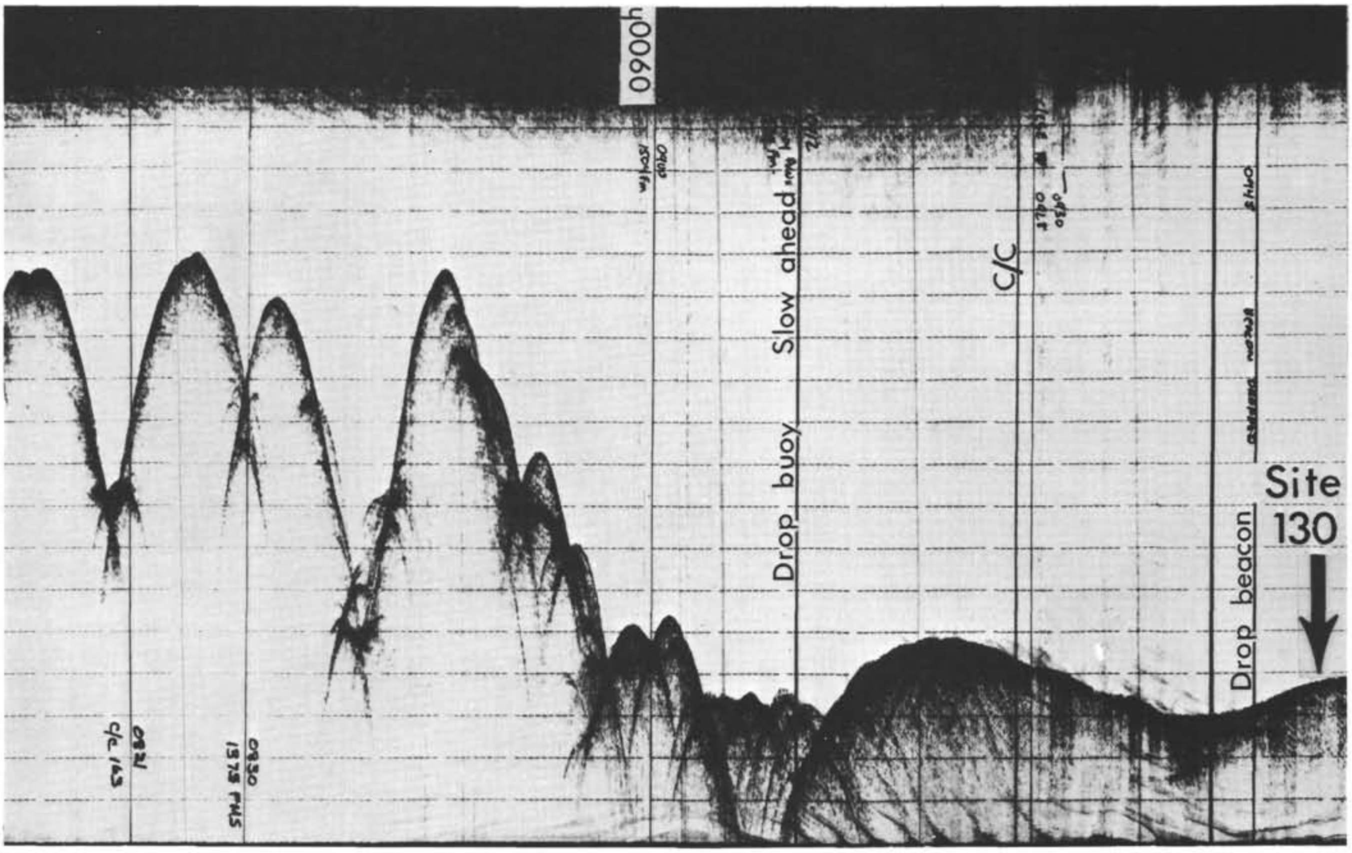

Figure 4. *(Continued)*

It is apparent from a glance at Column 2 of Figure 6 that the diversity of the fauna is related sympathetically to the inferred paleoclimate, with planktonic assemblages being more diversified in warm periods and less diversified in cold ones. A climatic cycle is observed in this core section starting with a warm-temperate climate at the base, passing to a cold-temperate climate at 14 to 16 cm and then to a warm climate again. Within the broad warm zone of the lower part of the section there occur three dark layers (e.g., 72, 115, 150 cm) of sapropel. These thin beds, with abundant pyrite and no benthic fauna, are interpreted to have been deposited under brief stagnant conditions during the climatic cycle. The cooling phase and cold maximum of the upper part of the core section contain no indication of reduced circulation or stagnation.

The climatic curve obtained from Core 130A-1-1 is very similar to the curve of the upper part of Albatross Core 189, studied by Parker (1958) and Olausson (1961), and recently reinterpreted by Ryan (1971). The presence of a tephra layer at 35 cm and the three sapropel layers below is similar to the section of Albatross Core 189 belonging to Climatic Zone 2 of Olausson (1961) which, according to the interpretation of Ryan (1971), is correlatable with Zone Y of Ericson (1961) and with the latest Pleistocene interglacial-glacial cycle (≈ 125,000 to 15,000 years B.P.). The tephra layer at 35 cm should correspond to the lower Santorini tephra layer of Ninkovich and Heezen (1965), which is now thought to have come from a prehistoric explosive volcanic eruption of the island of Ischia dated at about 25,000 years (Ninkovich and Hays, in press).

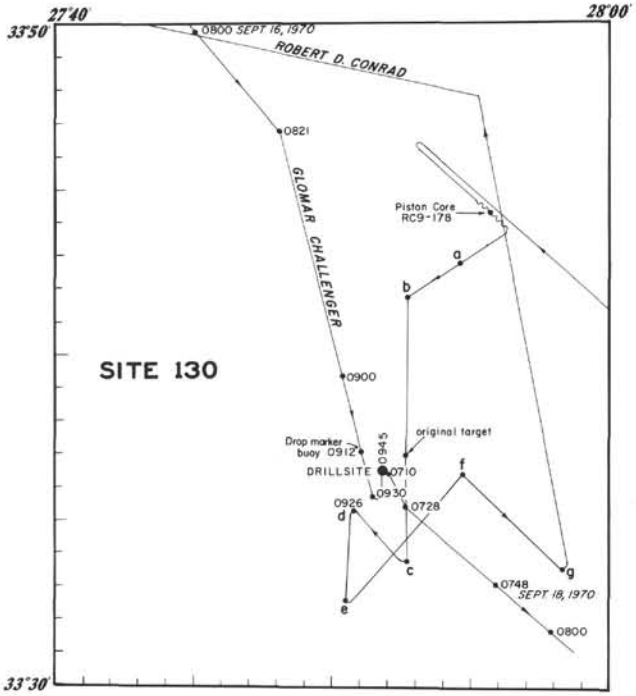

Figure 5. *Details of the* Glomar Challenger *site approach, showing the presite survey of the* Robert D. Conrad. *Lower case letters on the survey trace show the course changes depicted in Figure 2.*

TABLE 1
Core Inventory – Site 130

Core No.	No. Sections	Date	Time	Cored[a] Interval (m)	Cored (m)	Recovered (m)	Subbottom Penetration (m) Top	Bottom	Lithology	Age
Hole 130										
1	4	9/16	1845	3002-3012	10	5.1	13	23	Nanno ooze, sapropel, clay	Quaternary
2	3	9/16	2030	3038-3047	9	4.0	49	58	Nanno ooze, sapropel, clay	Quaternary
3	2	9/16	2200	3066-3075	9	2.0	77	86	Nanno ooze, sapropel, clay	Quaternary
4	2	9/17	0145	3127-3139	12	1.6	138	150	Clay, nanno ooze, sand	Quaternary
5	3	9/17	0540	3243-3252	9	3.5	254	263	Clay, nanno ooze, sand	Quaternary
6	5	9/17	1230	3400-3407	7	6.9	411	418	Clay, nanno ooze	Quaternary
CB1		9/17	1740	3407-3543	–	0.5kg	418	554	Clay, nanno ooze, sand	
7	CC	9/17	1910	3543-3552	9	0.1	554	563	Sandstone, cgl. marl	Quaternary
Total					55	23.2		563		
% Cored					9.7%					
% Recovered						42.1%				
Hole 130A										
1	1	9/18	0200	2922-3003	11	1.5	0	11	Nanno ooze	Quaternary
% Recovered						13.6%				

[a]Drill pipe measurements from derrick floor to sea floor

Similar paleontological investigations were conducted on Site 130 cores – Section 3 of Core 1 and Section 3 of Core 2. The climatic indications given by planktonic foraminifera are very uniform, ranging from temperate-warm to warm-temperate. Neither cold nor temperate intervals were recorded. Species which are now limited to subtropical areas, such as *Hastigerina pelagica, Globigerinoides conglobatus, G. sacculifer, Globigerina digitata, Candeina nitida* are common. Also, the number of species recorded is almost constant throughout the sections investigated. Twenty-seven other samples from Cores 1 to 3 were then investigated. The assemblages were found to be indicative of eutrophic or euxinic conditions. Again, they all indicate temperate-warm to warm-temperate conditions.

Since none of the assemblages was indicative of cold, or temperate-cold climate, it is possible that these sediments were deposited during the preglacial part of the Pleistocene. However, the lack of the nannofossil *Pseudoemiliania lacunosa* in Core 1 and the fact that it only appears in appreciable abundance in Core 3 and below, suggests that Cores 1 and 2 may belong to the *Gephyrocapsa oceanica* Zone. According to correlations established in Chapter 40.2, the lower boundary of this biozone is no older than about 1 my. Thus, it seems perhaps more probable that the materials recovered in Cores 1 and 2 were located by chance within interglacial stages of the late Pleistocene instead of within the preglacial early Pleistocene. The latter age assignment could make the very rich sapropel of Core 2, Section 3, 70-76 cm of Hole 130 time-equivalent to the prominent stagnation in Section 4, Core 1 of Hole 125.

According to Chapter 46, this episode of sapropel deposition, referred to as a Brunhes-Matuyama sapropel, is about 0.7 million years old, and establishes an average rate of sedimentation of ≈ 7 cm/10^3y for the sediment sequence down to and including Core 2.

As for the deeper part of the drilled section, if we assume that the bottom of the hole (563 meters) is close to the base of the Pleistocene or within the uppermost Pliocene, we then have for this interval more than 500 meters representing perhaps only some 1.2 million years. The calculated average rate of accumulation of $\approx$40 cm/10^3y is considerably greater than that of the surface sediments; this is not surprising considering that the deeper strata are mostly terrigenous clastics and that the hole terminated in a coarse-grained conglomeritic sandstone.

Pelagic sediments are limited, according to our evidence, to the uppermost part of the section, which represents the younger climatic cycles of the glacial Quaternary. Therefore, we may assume that only at that time was the Mediterranean Ridge raised above the abyssal plain to a height that could not thereafter be reached by bottom-transported clastics.

Planktonic Foraminifera (M.B.C.)

Planktonic foraminifera were found in abundance in all the samples investigated from Sites 130 and 130A.

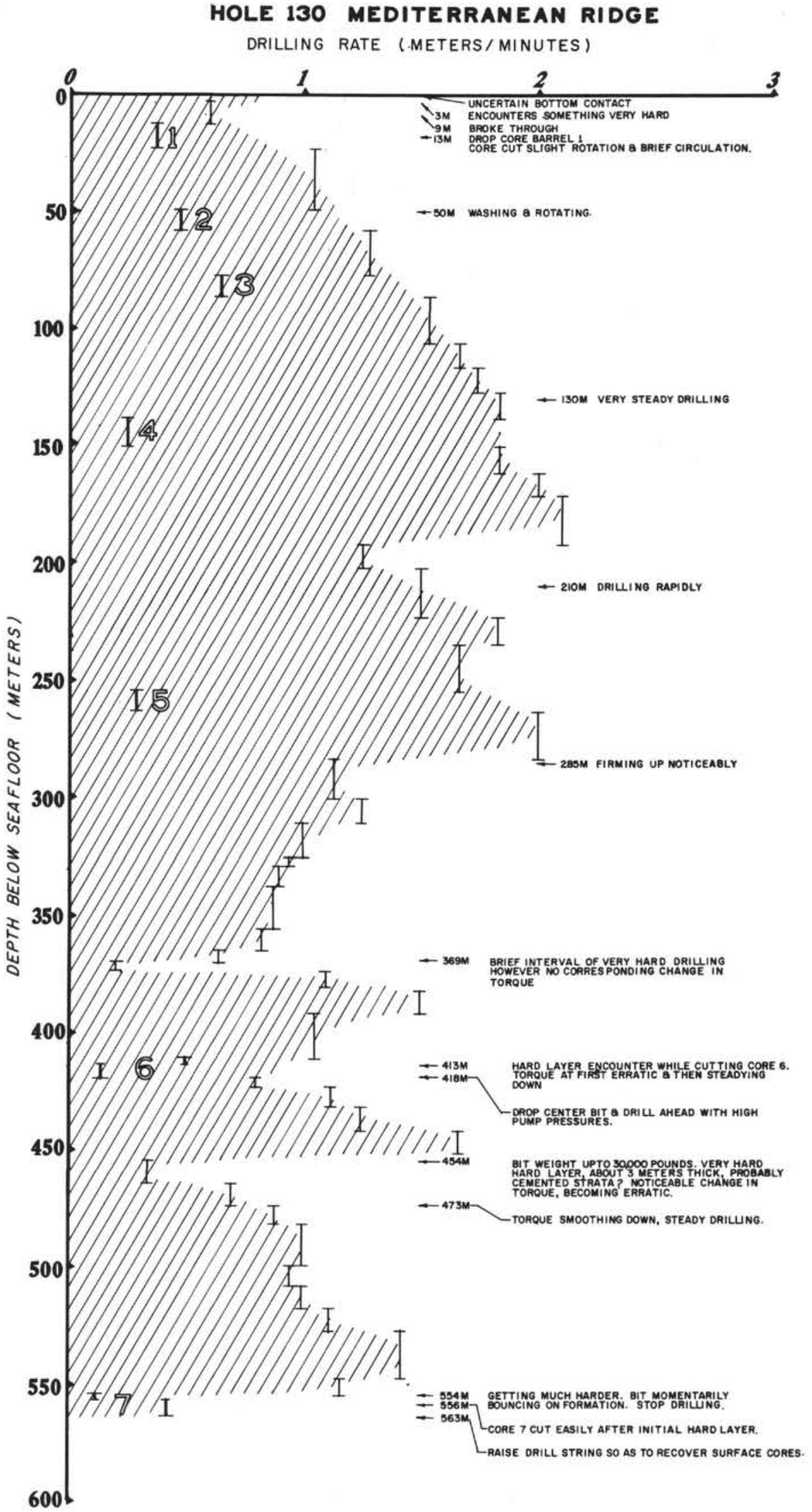

Figure 6. *Penetration rates during the drilling of Hole 130.*

TABLE 2
Distribution of Planktonic Foraminifera and Other Fossil Remains in the Late Quaternary Section of Hole 130A – Mediterranean Ridge

Depth Below Sea Floor (m)	Recovery (m)	Core Number	Section Number	Sample Interval (cm from Top)	Planktonic Foraminifera: *Globigerina*								*Globigerinoides*								*Globorotalia*								Other Genera						Various					
					bulbosa	*bulloides*	*digitata*	*eggeri*	*pachyderma*	*praedigitata*	*quinquelobata*	*rubescens*	*adriaticus*	*conglobatus*	*elongatus*	*helicinus*	*pyramidalis*	*quadrilobatus*	*ruber*	*sacculifer*	*acostaensis*	*dutertrei*	*inflata*	*obesa*	*oscitans*	*scitula*	*truncatulinoides*	s.p.	*Globigerinita glutinata*	*Globigerinita uvula*	*Hastigerina pelagica*	*Hastigerina siphonifera*	*Orbulina bilobata*	*Orbulina universa*	Pteropods	Pelecypods fragments	Otoliths	Ostracods	Organic matter	Pyrite
0	1-5	1	1	1-3	●	●		●	●		●		●			●	●		●	●		●	●			●	●	●	●		●	●		●	●					●
				14-16		●		●	●		●					●	●		●							●		●					○					○		
				23-25	●	●		●	●		●					●	●		●							●			●	●				●				○		
				30-32	●	●		●	●		●					●			●				●			●			●					●						
				43-45	●			●	●	●	●	●				●			●				●		●	●			●		○	○		●			○			
				56-58	●			●	●	●	●								●				●		●	●			●		●			●	○		○			
				72-74											○				○				○			○	○		○					○						
				90-92	●	●		●	●	●	●	●		●		●	●		●	●		●	●			●	●		●		●	●		●	○		○			○
				110-112	●	●	●	●	●	●	●	●			●		●		●		●	●	●			●	●	●	●			●	●	●					○	
				129-131	●	●	●		●	●	●				●	●			●				●			●			●		●	●		●	●		○			●
				147-150	●	●		●	●	●	●						●		●			●	●		●	●	●	●	●		●	●	●	●			○		●	
			CC	CC	●			●	●	●	●	●		●	●	●	●	●	●	●			●	●	●	●	●		●	●		●	●	●	●	○	○		●	●

However, some intervals from Cores 3 to 6 yielded only poor assemblages of immature or small-sized, possibly size-sorted specimens. Table 3 lists the ranges of planktonic foraminifera in 22 selected samples from Cores 1 to 7, Hole 130.

A few comments are added here. *Candeina nitida* is present as exceptionally rare specimens in Sample 130-1-3, 141-144 cm. As far as we know, this is the only record of this distinctly tropical species from the Mediterranean. It should be pointed out, however, that *Pulleniatina* is not present in this warm interval, though this genus has been recognized in the western Mediterranean (DSDP Core 134E, Side-wall Core 1).

The range of *Globorotalia truncatulinoides* appears to be restricted to the upper part of the Quaternary (no record below Core 2, Site 130) which is in agreement with the observations made at other sites in the Mediterranean.

Planktonic foraminifera are scattered in the terrigenous sediments of Cores 5 and 6, which yield a number of microfossils of different kinds, or of microscopic parts of larger organisms (see Table 3).

Reworking of pre-Quaternary planktonic foraminifera was noted below Core 6. These foraminiferal tests display different types of fossilisation and also show traces of erosion.

Benthonic Foraminifera (W.M.)

Benthonic foraminifera are sparse and never abundant in the Quaternary sequence penetrated in Holes 130 and 130A. The species identified are listed in Table 4.

Nannofossils (H.S.)

All cores and the center bit sample of Holes 130 and 130A contain Quaternary nannofossils in varying abundance. Light-colored layers of pelagic sediment contain abundant nannofossils, while in the sapropels, nannofossils, along with diatoms and sponge spicules, are rare (130-3, CC and 130-4, CC). All samples show some degree of reworking from older sediments. In Cores 130-6 to 130-7 the abundance of *Discoaster brouweri* leads to the conclusion that there must have been massive transport of Upper Pliocene sediments by turbidity currents or subaquatic slumping to account for the presence of such allochthonous, heterochronous nannofossils. If the abundant *Discoaster brouweri* flora is autochthonous, these cores would have to be dated as latest Pliocene.

Cores 130-1 and 130A-1 are remarkable by containing an assemblage with *Discoaster perplexus* and *Oolithotus antillarum*, which in the Mediterranean have hitherto been only encountered south and southeast of Crete. This assemblage is also represented in the sample of Station No. 77 of the 2nd Austrian Deep Sea Expedition of the SMS Pola, 13 August, 1891 (lat. 34° 37′20″ long. 26° 33′30″, depth 3310 m). *Gephyrocapsa oceanica* also is abundant in these upper cores, while large specimens of *Braarudosphaera bigelowi* are characteristically present in Core 3. From Core 3 to Core 7 *Pseudoemiliania lacunosa* is the dominant coccolith. An interval of lowered frequency of nannofossils occurs in Cores 4 and 5.

The age-diagnostic nannofossil assemblages are listed below.

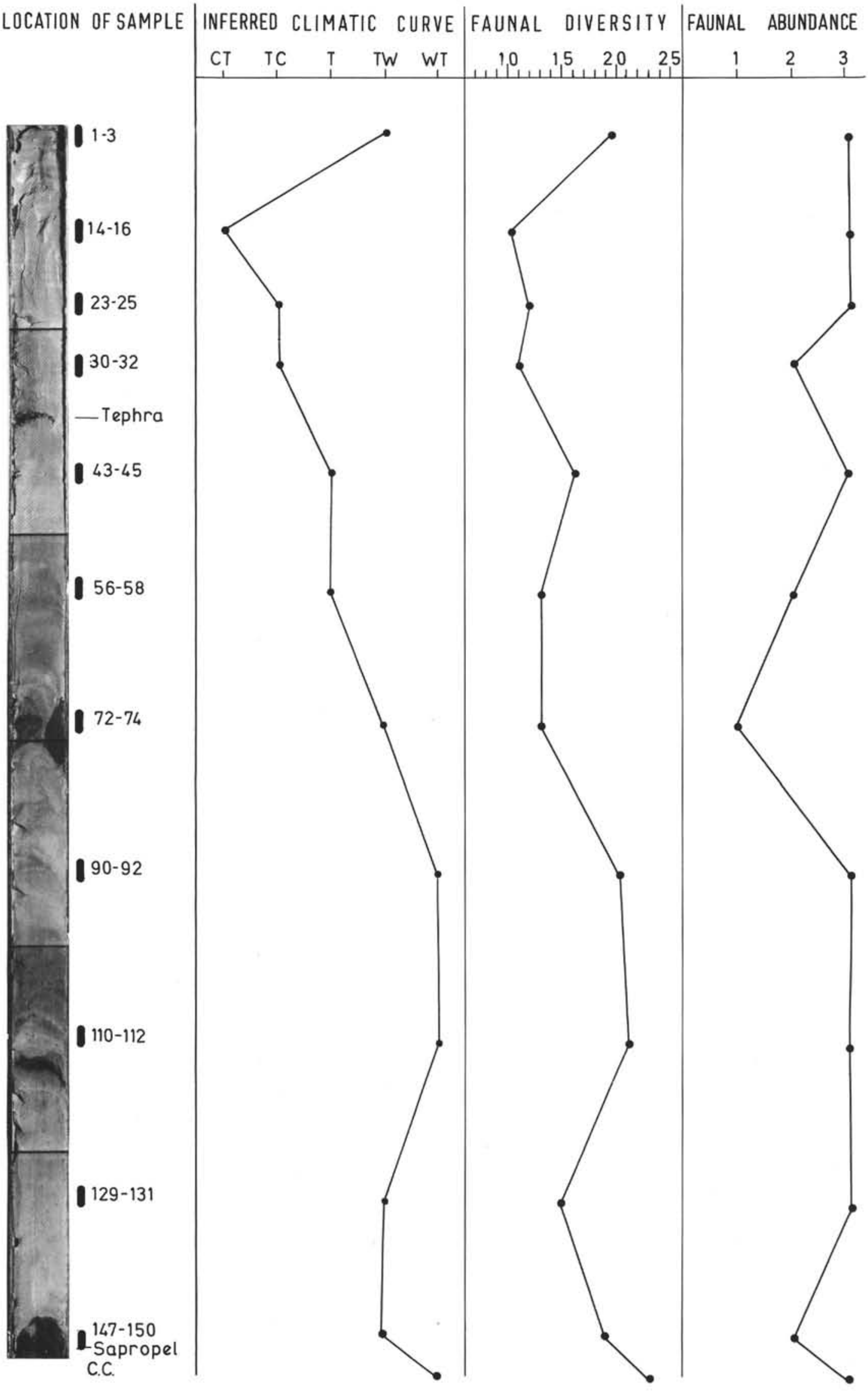

Figure 7. *Climatic interpretations of selected samples from Section 1, Core 1 of Hole 130A. For a discussion of the respective curves, see text.*

TABLE 3

Distribution of Planktonic Foraminifera and Other Fossil Remains in the Quaternary Section of Hole 130

Depth Below Sea Floor (m)	Recovery (m)	Core Number	Section Number	Sample Interval (cm from Top)	Planktonic Foraminifera: *Globigerina*								*Globigerinoides*										*Globorotalia*							Other Genera								Other Fossils											Various		
					bulbosa	*bulloides*	*eggeri*	*falconensis*	*pachyderma*	*praedigitata*	*quinqueloba*	*rubescens*	*adriaticus*	*conglobatus*	*elongatus*	*helicinus*	*pyramidalis*	*quadrilobatus*	*ruber*	*sacculifer*	*tenellus*	*trilobus*	*acostaensis*	*crassaformis*	*dutertrei*	*inflata*	*obesa*	*scitula*	*truncatulinoides*	s.p.	*Candeina nitida*	*Globigerinita glutinata*	*G. uvula*	*Hastigerina siphonifera*	*Orbulina bilobata*	*O. suturalis*	*O. universa*	Pteropods	Pelecypods fragments	Otoliths	Siliceous sponge spicules	Organic matter	Ostracodes	Radiolaria	Spores	Holoturian sclerites	Tunicates micrascidites	Histricophaerids	Pyrite	Pelagic sedimentation	Terrigenous sedimentation
13			1	117-120	●	●		●	●	●	●	●			●	●	●	●	●	●			●			●	●	●		●		●		●	●		●			○										X	
			2	101-103																			●		●	●				●				●	●		●					○								X	
	5	1	3	141-143	●	●		●	●	●	●	●			●	●	●		●							●	●	●		●	●	●		●	●		●					○							○	X	
			4	136-139	●	●			●		●	●				●	●		●							●								●			●			○										X	
23			CC	CC	●	●	●	●	●	●	●	●			●			●	●							●		●				●					●	○											○	X	
49			1	59-61	●	●			●		●	●	●		●	●			●	●					●	●		●	●	●		●					●												○	X	
			2	148-150	●	●			●		●	●		●			●	●	●	●	●	●			●	●		●				●		●			●													X	
			3	63-65	●	●		●	●	●	●	●		●	●				●							●	●	●				●		●			●			○									○	X	
58			CC	CC	●	●		●	●		●		●	●	●	●	●	●	●			●				●	●	●				●		●			●			○									●	X	
77			1	130-132	○	○					○	○																○				○	○									○	○	○		○	○	○			X
	1.7	3	2	23-25	●	●								●	●	●	●		●						●	●	●							●			●	●	●	○										X	
86			CC	CC		○		○	○		○			○	○			○	○							○						○		○			○												○		X
138 150	1.6	4	2	94-97	●	●		●	●	●	●	●	●	●	●	●	●		●	●	●					●		●		●		●		●			●													X	X
259			2	71-74		○		○	○		○	○							○									○				○		○								●							○	X	X
	3.5	5	3	30-33		○			○		○														○	○				○							○					●									X
263			CC	CC	●	●	●		●		●			●	●				●			●	●			●						●		●			●	○	○			○							○	X	X
411			2	90-93	●	●		●	●		●	●			●	●			●													●					●		○	○				○			○				
			3	70-74	○				○		○	○																○				○	○								○	○			○						X
	6.9	6	4	69-72	○				○		○	○																○												○		●	○	○		○					X
			5	83-85	○	○			○			○																○				○	○								○	●		○							X
418			CC	CC		●		●	●		●			●	●				●	●						●		●		●		●					●												○		X
563	0.1	7	CC	CC					●		●				●				●	●				●		●											●												○		X

TABLE 4
Range Distribution of the Benthonic Foraminifera in Hole 130 – Mediterranean Ridge

Age	Depth Below Sea Floor (m)	Cores	*Karreriella bradyi* (Cush.)	*Pyrgo depressa* (d'Orb.)	*Articulina tubulosa* (Seg.)	*Cibicides pseudoungerianus* (Cush.)	*Rotalia perlucida* Herr. All. & Earl.	*Eponides* cf. *haidingeri* (Brady)	*Eponides umbonatus* (Reuss)	*Pullenia bulloides* (d'Orb.)	*Gyroidina soldanii* (d'Orb.)	*Bulimina* cf. *gibba* Forn.	*Bulimina pupoides* d'Orb.	*Pleurostomella alternans* Schwag.	*Spirillina vivipara* Ehrenbg.	*Nodosaria* cf. *longiscata* d'Orb.	*Parafrondicularia advena* (Cush.)	*Cassidulina crassa* d'Orb.	*Bolivina catanensis* Seg.	*Bolivina dilatata* Reuss	*Bulimina* cf. *affinis* d'Orb.	*Valvulineria bradyana* (Forn.)	*Cassidulina carinata* Silv.	*Nonionella turgida* (Will.)	*Bolivina pseudoplicata* Herr. All. & Earl.	*Uvigerina peregrina-mediterranea*	*Discorbis* cf. *globularis* (d'Orb.)	*Angulogerina angulosa* (=carinata)	*Neoconorbina terquemi* (Rzehak)	*Nonion* cf. *padanum* Perconig	*Ammonia beccarii* (Linn.)	*Cibicides floridanus* (Cush.)	*Gyroidina* cf. *neosoldanii* Brotzen	*Epistomina elegans* (d'Orb.)
	Sea Floor 2979 m																																	
Pleistocene	13-23	1	x	x	x	x	x	x	x	x	x	x	x																					
Pleistocene	49-58	2			x									x																				
Pleistocene	77-86	3												x	x																			
Pleistocene	138-150	4							x		x					x	x	x																
Pleistocene	254-263	5			x														x	x	x	x	x	x										
Pleistocene	411-418	6																x		x			x		x	x	x	x	x	x				
Pleistocene	418-554	CB1				x																								x	x	x	x	x
Pleistocene	554-563	7																		x														

Quaternary

Samples: 130-1-1, 148 cm; 130-1-2, 28 cm; and 130-1-3-140 cm:

Coccolithus pelagicus
Ceratolithus cristatus
Cyclococcolithus leptoporus
Gephyrocapsa oceanica
Heliscosphaera carteri
Micrascidites sp.
Rhabdosphaera clavigera
Rhabdosphaera stylifera
Pontosphaera scutellum
Scyphosphaera apsteini
Syracosphaera pulchra
Thoracosphaera imperforata

In samples 130-1-4, 14 cm and 130-1, CC, there are also:

Discoaster perplexus
Oolithotus antillarum
Scapholithus fossilis
Umbilicosphaera mirabilis

Reworked nannofossils: A few Pliocene discoasters.

Samples: 130-2-1, 48 cm, 130-2-2, 76 cm; 130-2-3, 56 cm; and 130-2, CC:

Braarudosphaera bigelowi
Ceratolithus cristatus
Coccolithus pelagicus
Cyclococcolithus leptoporus
Gephyrocapsa oceanica
Helicosphaera carteri
Pontosphaera japonica
Pontosphaera multipora
Pontosphaera scutellum
Pseudoemiliania lacunosa
Rhabdosphaera clavigera
Rhabdosphaera stylifera
Scyphosphaera apsteini
Syracosphaera pulchra
Thoracosphaera imperforata
Umbilicosphaera mirabilis

Reworked: Rare Pliocene discoasters (*D. pentaradiatus*) and some Eocene discoasters (*D. barbadiensis*).

Samples: 130-3-2, 89 cm; 130-3-2, 103 cm; and 130-3, CC:

Braarudosphaera bigelowi (large specimens)
Ceratolithus cristatus
Coccolithus pelagicus
Cyclococcolithus leptoporus
Gephyrocapsa oceanica
Helicopontosphaera carteri
Lithostromation perdurum
Micrascidites sp.
Pontosphaera japonica
Pontosphaera scutellum
Rhabdosphaera clavigera
Rhabdosphaera stylifera
Reticulofenestra pseudoumbilica
Scyphosphaera apsteini

Sphenolithus abies
Thoracosphaera imperforata

Reworked: Pliocene and Miocene discoasters.

Samples: 130-4-2, 96 cm; 130-4-2, 125 cm:
Braarudosphaera bigelowi
Ceratolithus telesmus
Coccolithus pelagicus
Cyclococcolithus leptoporus
Gephyrocapsa oceanica
Helicosphaera carteri
Lithostromation perdurum
Pontosphaera japonica
Pontosphaera scutellum
Pseudoemiliania lacunosa
Rhabdosphaera stylifera
Scyphosphaera apsteini
Scyposphaera pulcherrima
Syracosphaera pulchra

In 130-4, CC, there are plenty of diatoms and sponge spicules, but also some nannofossils of similar assemblage as in Section 2.

Reworked: *Discoaster barbadiensis* and few other discoasters.

Sample: 130-5-2, 60 cm: barren

Samples: 130-5-3, 100 cm and 130-5, CC:
Poor assemblage with:
Coccolithus pelagicus
Cyclococcolithus leptoporus
Gephyrocapsa oceanica
Pontosphaera scutellum

Samples: 130-6-1, 128 cm; 130-6-2, 140 cm; 130-6-3, 139 cm; 130-6-4, 110 cm; 130-6-5, 120 cm; 130-6, CC:
Braarudosphaera bigelowi
Coccolithus pelagicus
Cyclococcolithus leptoporus
Gephyrocapsa oceanica
Helicosphaera carteri
Discolithina macropora
Lithostromation perdurum
Pontosphaera japonica
Pseudoemiliania lacunosa
Rhabdosphaera clavigera
Rhabdosphaera stylifera
Scapholithus fossilis
Scyphosphaera apsteini and *Scyphosphaera pulcherrima*
Syracosphaera pulchra
Thoracosphaera sp.

Discoaster brouweri, also its three-radiate and four-radiate form are rather abundant, so that is appears rather dubious, whether they were all reworked. There is also *Discoaster challengeri* (rare), *Discoaster barbadiensis*, overcalcified discoasters and lots of *Micrascidites*.

Sample: 130-CB:
Braarudosphaera bigelowi
Ceratolithus cristatus
Coccolithus pelagicus
Cyclococcolithus leptoporus
Discolithina macropora
Helicosphaera carteri
Micrantholithus vesper
Micrascidites sp.
Pontosphaera japonica
Pontosphaera scutellum
Pseudoemilia lacunosa
Rhabdosphaera stylifera
Scyphosphaera apsteini
Syracosphaera pulchra
Thoracosphaera heimi

Reworked discoasters common (*D. brouweri*).

Samples: 130-7-1, 1 cm and 130-7, CC:
Poor assemblages with:
Braarudosphaera bigelowi
Coccolithus pelagicus
Cyclococcolithus leptoporus
Pseudoemiliania lacunosa
Pontosphaera japonica
Pontosphaera scutellum
Scyphosphaera absteini
Thoracosphaera imperforata

Samples: 130A-1-1, 1 cm; 130A-1-1, 118 cm; and 130A-1, CC:
Nannofossil-assemblage with the characteristic
Discoaster perplexus and
Oolithotus antillarum, also:
Braarudosphaera bigelowi
Ceratolithus cristatus
Coccolithus pelagicus
Cyclococcolithus leptoporus
Emiliania huxleyi
Gephyrocapsa oceanica
Helicosphaera carteri
Micrascidites sp.
Pontosphaera scutellum
Rhabdosphaera clavigera
Rhabdosphaera stylifera
Scyphosphaera apsteini
Syracosphaera pulchra
Scapholithus fossilis
Thoracosphaera heimi
Umbilicosphaera mirabilis

Sample: 130A-1-1, 35 cm (Tephra) with few nannofossils of the same assemblage, also in 130A-1-1, 70 cm.

LITHOSTRATIGRAPHY

The section of Site 130 consists of two lithologic units. The upper unit (Unit 1) (see Table 5) consists of light buff-colored foraminiferal marl of pelagic origin, containing three thin beds of sapropel and a single thin layer of volcanic tephra. The lower unit (Unit 2) is comprised mostly of dark-colored carbonate-poor muds believed to be of turbidity current origin, with only thin interbeds of pelagic foraminiferal marl and sapropel.

The contact between the two lithologic units has been placed at 14.5 meters below bottom, at the top of the first dark mud layer encountered (i.e. at 3 cm in Core 1, Section 2, of Hole 130).

TABLE 5
Lithologic Units of Holes 130 and 130A

Unit	Lithology	Age
1	Pelagic foraminiferal marl ooze, sapropel, tephra.	Quaternary
14.5		
2	Terrigenous black muds, sands, and sandstones, mainly turbidites, with intercalated foraminiferal marl ooze and sapropel.	Quaternary
563		

Unit 1 – Pelagic Foraminiferal Marl Ooze

The light yellowish brown and light gray, homogeneous, plastic marl oozes recovered in Core 1 of Hole 130A (0-11m) and Section 1, Core 1 of Hole 130 (13-14.5m) are mainly composed of nannofossils, foraminifera, and fine-grained mineral components (quartz, clays and pyrite). Carbonate content ranges from 45 to 75 per cent. The boundaries between the tan and gray units, which range from 10 to 30 cm in thickness, are well defined. Burrowing and hydrotroilite spots or bands are often apparent, and they have a characteristic H_2S odor.

Three beds of sapropel occur at 70 to 75 cm, 102 to 104 cm, and 143 to 150 cm, in Core 1 of Hole 130. A single thin layer of brown volcanic tephra appears in the same core section at 35 cm, and consists almost entirely of clear, colorless glass shards with an index of refraction of 1.52 and a grain size of about 50 microns.

The sediments of Unit 1 have the appearance of a normal pelagic facies that was deposited principally through particle-by-particle settling in a tranquil environment.

Unit 2 – Terrigenous Black Muds, Sands, and Sandstones

Between 14.5 and 563 meters the dominant lithology is black mud with intercalations of light pelagic marl ooze (see Figure 8A) and occasional sapropel beds. Some of the dark mud layers are graded, with a lamina of silt or sand at the base. Discrete sand layers (Figure 9) are observed in the lower part of the unit, and are generally 10 to 15 cm thick; they grade upward into silts and clays.

The muds are plastic, homogeneous and dark gray to blue black in color. They are laminated and semi-indurated in Core 5, at 250 meters, and are hard and shaly in Core 6. Terrigenous components predominate in the fine-grained muds, including clay minerals (mainly montmorillonite), quartz, mica, some pyrite, and dolomite. The calcium carbonate content is very low, less than 5 per cent in all the samples examined.

The sand grains are land derived, composed mainly of rounded, frosted and unfrosted quartz (75%), plagioclase (3%), chlorite (2%), green hornblende (10%), epidote (3%), and some authigenic pyrite (0-2%). For a more detailed description of their mineralogy see Chapter 25.2.

The lower contacts of the dark layers are always sharp (Figure 8B), while their upper contacts may show a transition to a lighter color. The base of one dark layer occasionally truncates another layer. The tops of these

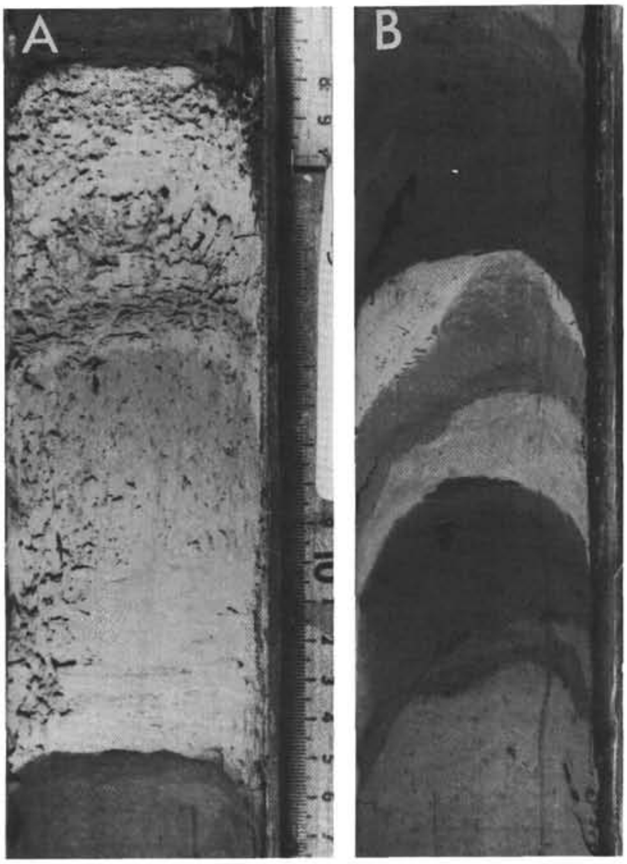

Figure 8. *Examples of pelagic marl ooze layers intercalated in dark terrigenous muds in Section 2, Core 2 of Hole 130. 'A' illustrates a relatively thick interval at 98 to 115 cm. Note the sharp bedding contacts. 'B' shows much thinner intervals of various light-colored shades and traces of burrow-mottling of the light sediment exclusively within the upper parts of the terrigenous layers. These high carbonate marl oozes layers are interpreted as background pelagic sedimentation between episodes of rapid terrigenous mud accumulation. Scale is in centimeters.*

layers are often speckled with light-colored foraminiferal marl oozes carried down from an overlaying pelagic deposit by burrowing mud eaters (Figure 10). The graded sands at the base and traces of erosion on the basal contact lead us to interpret the dark muds as turbidites.

The interbedded pelagites are light-colored, gray, greenish, or brownish yellow marl oozes. They display the same lithologic makeup as the pelagic oozes of Unit 1. In the upper part of the turbidite sequence, the marl oozes generally consist of thin (5-10 cm), and occasionally thicker (30-40 cm) layers, all with sharp contacts. Toward the base of the hole, a 6 meter-thick sequence of the pelagic marls occurs (413-419 m).

In Cores 5 and 6 quartzose sandstones were penetrated. Their petrographic composition (see Chapter 25.2) is similar to that of the sands and they can be interpreted as a deep-sea turbidite deposit.

The oldest Quaternary sediments penetrated include pebble-sized clasts which are generally assigned by sedi-

Figure 9. *Illustration of a graded sand interval at the base of a terrigenous mud layer in Section 2, Core 2 of Hole 130. Such basal layers are usually poorly sorted and occasionally finely laminated. Some evidence of scour or winnowing at the basal contact is seen. For example, the pocket of sand seen just above the 140 cm marking is perhaps the filling of a groove or flute depression.*

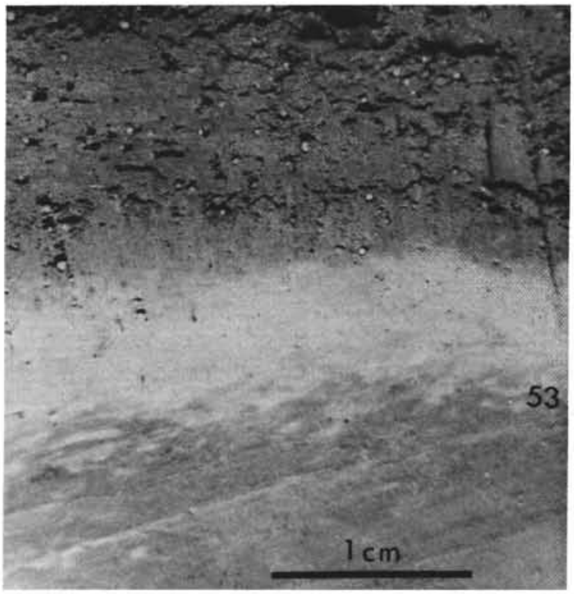

Figure 10. *Burrow markings (bioturbation) of light colored pelagic sediment (53 cm) in the upper part of a terrigenous mud layer are interpreted as an indication that a significant period of time elapsed for the deposition of the calcareous-rich sediment facies. A sharp upper contact (52 cm) is evidence of an abrupt interruption with the rapid emplacement of terrigenous mud. The scattered tests of foraminifera in the overlying mud layer are believed to have been eroded from a pelagic ooze substratum during passage of a sediment-laden turbidity current and left as a residual slag deposit in the basal section of the mud layer.*

mentologists to a proximal depositional setting. Finer-grained younger turbidites have the textural appearance of a more distal environment and the youngest are interbedded with a microbreccia of mixed biogenic and terrigenous components (Figure 11) indicating the presence of nearby uplifted pelagic deposits.

PHYSICAL PROPERTIES

Although Hole 130 was drilled to 563 meters, physical measurements of the properties were determined only on the first six cores recovered, above a depth of 418 meters. The succession includes nannofossil oozes and terrigenous black clays with occasional fine layers of sand or silt. Trends downhole within this sequence of relatively uniform lithology are readily recognizable.

Penetrometer readings vary between 113.0 and 1.7 x 10^{-1} mm, and there is a steady decrease in penetratability with depth. An inverse correlation with bulk density values was also noted.

Bulk densities lie in the range of 1.45 to 1.95 gm/cc, and grain densities in the range of 2.07 to 2.58 gm/cc. There is a steady increase with depth. Water content and porosity vary between 43.2 and 20.6 per cent and 63.8 and 39.8 per cent, respectively, decreasing also with depth.

Natural gamma counts vary from 1800 to 3200 counts, and appear to increase slightly with depth, if an average value for each core is taken. For example, in the lower cores, 5 and 6, there are no readings of less than 2200, and most lie between 2500 and 3000 counts. This increase is accompanied by decreasing porosity, so that the actual radiation per unit volume of mineral grains is not greatly different. Sapropel beds produce higher count rates, around 3000. Sand layers give counts of 2500 to 2900. Layers with a great concentration of forams, and hence a higher calcium carbonate content, correspond to low count rates of around 2000.

SUMMARY AND CONCLUSIONS

The dark-colored low-carbonate terrigenous muds, sands and sandstones of Lithologic Unit 2 are interpreted according to their sedimentary textures and primary bedding structures as the depositional products of turbidity currents. Assuming that this facies identification is correct, we are permitted then to speculate that the vast amount of the section drilled at Site 130 was originally deposited in a basinal setting.

The disturbed configuration of the strata of the Mediterranean Ridge is introduced here as evidence of a youthful phase of geological activity that deformed what was once believed to be horizontally bedded "flysch-like" detrital

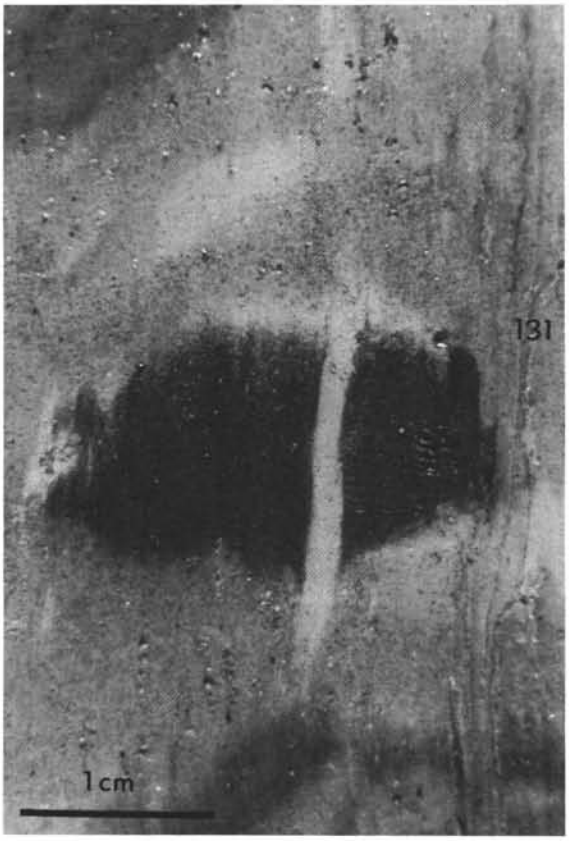

Figure 11. *Sedimentary micro-breccia in Section 1, Core 1 of Hole 130. Note the trace of a burrowing organism through the central dark-colored terrigenous mud clast in the breccia. indicating that the structures of this deposit are primary and are not the result of an artificial drilling disturbance.*

layers. We note that subsurface stratified reflectors are seen in the lesser-deformed regions of the ridge and that this type of acoustic reflectivity is generally characteristic of the flat-lying modern abyssal plains of the ocean basin floor (Ewing and Ewing, 1971).

As to the age of the initiation of the sedimentary deformation of the Mediterranean Ridge, we offer the following observations.

1) A sedimentological gradient exists in the terrigenous sequences of lithologic Unit 2. The lower strata of Cores 3 through 7 contain significantly more sand, thicker basal intervals in each turbidite bed, and thinner upper pelitic intervals than those found in Cores 1 and 2. In fact, the coarsest grain-size fractions were seen in the conglomeratic sandstone of the lowermost core. Nearer the top of the recovered section the average thickness of each terrigenous mud interval increases, sand-sized clastics disappear altogether, and the basal contacts of each graded interval often contain only a single millimeter-thick lamina of fine sand or silt.

2) At the very top of Section 1 of Core 1 a sedimentary microbreccia appears with mud clasts involving the dark terrigenous muds mixed with clasts of pelagic marl ooze. We infer that there must have been some nearby topographic elevation in the basin from which the mud slid in order to form these slump deposits. Yet, an enigma remains concerning how terrigenous sediments coming into the basin by gravity-propelled turbidity currents could have carried their suspended terrigenous mud load to the surface of such a topographic high.

3) The superficial layers (0-14.5 m) of the Mediterranean Ridge at the drill site are made up only of sediments of pelagic origin.

A sedimentologist confronted with the above observations and inferences might interpret an evolution of the depositional environment from that of an original by proximal basinal setting to that of a distal basinal setting, and finally to a setting completely removed from the basin itself. However, in light of the recognized deformation of the Mediterranean Ridge, it is also possible to envision perhaps a gradual uplift of a once basinal sedimentary province to an elevation where only finer and finer sediments were able to reach the local sea bed. Within the framework of a deformational model, it is possible to imagine the buckling up of parts of the abyssal plain as a mechanism for introducing recycled terrigenous clastics as components in subaqueous slumps. The sedimentological gradient previously discussed can be viewed as a manifestation of gradual tectonism, with a decrease in the sand fraction in the turbidite layers signaling the first phases of uplift and the superficial strata heralding the complete vertical isolation of this part of the ridge from turbidity current deposition. If the pelagic ooze/terrigenous mud contact is at 14.5 meters below bottom, and the accumulation rate for the pelagic sediments is assumed to be ≈ 3 cm/10^3y (a value comparable to that observed in the pelagic sequences of Site 125, also on the Mediterranean Ridge), then the time represented for the blanket of pelagic marl oozes amounts to about 480,000 years.

However, regardless of the details of the timing of the tectonism, the above arguments when coupled with evidence of fresh faults scarps on the sea bed (bottom photographs) and the broken up nature of the sea floor relief all corroborate that the reorganization of this central region of the eastern Mediterranean is remarkably youthful. Furthermore, the contemporary earthquake seismicity (Comninakis and Papazachos, in press) strongly suggests continuing uplift and buckling.

The great thickness of the Pleistocene terrigenous sequence indicates that there was a former abyssal plain province of some magnitude in the Levantine Basin prior to the formation of the Mediterranean Ridge. Unless there has been extensive intrabasinal underthrusting and/or crustal shortening, it is likely that the sedimentary accumulations of this basin formed as a continuous seaward extension of the submarine Nile Cone distributory system. In fact, mineralogical investigations of both the fine- and coarse-grained terrigenous minerals of lithologic Unit 2 reported in Chapter 25.2 support this conclusion by showing a marked similarity of the Site 130 mineral assemblages and those of a subsequent drill site (131) on the lower Nile Cone, as well as those of the subsurface Nile River bed itself.

Although it is premature to comment further on the Nile provenance, without presenting the results of Site 131 (see following chapter), it suffices to conclude that the markedly thick wedge of post-Reflector-M strata drilled at

Site 130 consists to a great extent, of terrigenous components derived from Africa.

As to the nature of the tectonism which deformed the former sedimentary basin, we offer two hypotheses which are discussed further in Chapter 49 of this volume. In keeping with the scope of this Site Report we shall only comment that the first hypothesis involves basement thrusting (e.g., the thrust-wedges of Dewey and Bird, 1970) related to the interaction of the African and Aegean lithospheric plates during the late Cenozoic approach of Africa and Eurasia (McKenzie, 1970; Lort, 1971; and Smith, 1971); and that the second hypothesis raises the question of the role played by plastic flow of a subsurface layer of salt, known to have been deposited in the eastern Mediterranean basins during the late Miocene, and confirmed from gradients in the ionic composition of interstitial waters (see Chapter 31) in the subsurface Mediterranean Ridge proper.

REFERENCES

Bremer, H., 1971. Geology of the coastal regions of southwestern Turkey. **In** *Geology and History of Turkey* (Ed. A. S. Campbell). The Petroleum Exploration Society of Libya, Tripola, Libya. 257.

Butzer, K. W. and Hansen, 1965. On the Pleistocene evolution of the Nile Valley in Southern Egypt. *The Canadian Geogr.* **9** (2).

Caputo, M., Panza, G. F. and Postpischl, D., 1970. Deep Structure of the Mediterranean basin. *J. Geophys. Res.* **75**, 4919.

Chumakov, I. S., 1967. Pliocene and Pleistocene deposits of the Nile Valley in Nubia and Upper Egypt. *Acad. Sci. USSR, Geol. Inst.* "Nauka," Moscow. 1.

Dewey, J. F. and Bird, J. M., 1970. Mountain belts and the new global tectonics, *J. Geophys. Res.* **75** (14), 2625.

Elgabaly, M. M. and Khadar, M., 1962. Clay mineral studies of some Egyptian desert and Nile alluvial soils. *J. Soil Sci.* **13**, 333.

Emelyanov, E. M., 1968. Mineralogy of the sand-silt fraction of recent sediments of the Mediterranean Sea, Lithology and Mineral Resources, p. 127-142 (a translation from *Litologyia i Poleznye Iskopaemye,* (2), 3.

Emery, K. O., Heezen, B. C. and Allan, T. D., 1966. Bathymetry of the eastern Mediterranean Sea. *Deep-Sea Res.* **13**, 173.

Ericson, D. B., 1961. Pleistocene climate record in some deep-sea sediment cores. *Annals of the New York Academy of Science.* **95**, 537.

Ewing, J. and Ewing, M., 1971. Seismic reflection. **In** *The Sea.* (Ed. A. E. Maxwell), John Wiley and Sons. **4** (1), 1.

Giermann, G., 1966. Gedanken zur Ostmediterranen Schwelle. *Bull. Inst. Oceanogr. Monaco.* **66**, 1.

_______, 1968. The eastern Mediterranean ridge. Rapp. Comm. Int. Mer. Medit. **19** (4), 44.

Goncharov, V. P. and Mikhaylov, O. V., 1963. New data concerning the topography of the Mediterranean Sea bottom. *Okeanologiya.* **3**, 1056.

Hersey, J. B., 1965. Sedimentary basins of the Mediterranean Sea. **In** *Submarine Geology and Geophysics.* (Eds. W. F. Whittard and R. Bradshaw), Proc. 17th Symposium Colston Res. Soc., Apr. 5-9, Butterworth, London, 75.

Lort, J. M., 1971. The tectonics of the eastern Mediterranean; A geophysical review. *Reviews of Geophysics and Space Physics.* **9** (2), 189.

McKenzie, D. P., 1970. Plate tectonics of the Mediterranean Region. *Nature.* **226**, 239.

Mikhaylov, O. V., 1965. The relief of the Mediterranean Sea bottom. **In** *Basic features of the geological structure, of the hydrologic regime and biology of the Mediterranean Sea.* Fomin, L. M., (Editor). Science Publ. House, Moscow. 10.

Moskalenko, V. N., 1966. New data on the structure of the sedimentary strata and basement on the Levant Sea. *Oceanologiya.* **6**, 828.

Ninkovich, C. D. and Heezen, B. C., 1965. Santorini tephra, **In** *Submarine Geology and Geophysics.* W. F. Whittard and R. Bradshaw, Eds., Butterworth, London. 413.

Ninkovich, C. D. and Hays, J. D. (in press). Tectonic setting of Mediterranean volcanoes. *Acta of the International Scientific Congress on the Volcano of Thera.* Athens, Greece, Sept. 15-23, 1969.

Olausson, E., 1961. Studies of deep-sea cores. *Rep't Swedish Deep Sea Exped. 1947-1948.* **VIII**, 337.

Papazachos, B. C. and Comninakis, P. E., 1971. Geophysical and tectonic features of the Aegean Arc. *J. Geophys. Res.* **76**, 8517.

Parker, F. L., 1958. Eastern Mediterranean foraminifera. *Rep't Swedish Deep-Sea Exped. 1947-1948, Vol.* **VIII**, 219.

Payo, G., 1967. Crustal structure of the Mediterranean Sea by surface waves. Part I; group velocity. *Bull. Seismol. Soc. Am.* **57**, 151.

Rabinowitz, P. D. and Ryan, W. B. F., 1970. Gravity anomalies and crustal shortening in the eastern Mediterranean. *Tectonophysics.* **10**, 585.

Ryan, W. B. F., 1971. Stratigraphy of Late Quaternary sediment in the eastern Mediterranean. **In** *Sedimentation in the Mediterranean Sea.* D. J. Stanley (Editor), Smithsonian Press, Washington, D.C.

Ryan, W. B. F., Stanley, D. J., Hersey, J. B., Fahlquist, D. A. and Allan, T. D., 1971. The tectonics and Geology of the Mediterranean Sea, **In** *The Sea.* Maxwell, A. (Editor), John Wiley and Sons, New York. **4**, 387.

Smith, A. G., 1971. Alpine deformation and the oceanic areas of the tethys, Mediterranean, and Atlantic. *Bull. Geol. Soc. Am.* **82**, 2039.

Sukhri, N. M., 1950. The mineralogy of some Nile sediments. *Geol. Soc. London* Q. J. **105**, 513; **106**, 466.

_______, 1951. Mineral analyses tables of some Nile sediments. *Bull. Inst. Fouad 1-er du desert.* **1**, 2.

Van der Kaaden, G., 1971. Basement Rocks of Turkey. **In** *Geology and History of Turkey.* A. S. Campbell (Editor). The Petroleum Exploration Society of Libya, Tripoli, Libra. 119.

Venkatarathnam, K. and Ryan, W. B. F., 1971. Dispersal patterns of clay minerals in the sediments of the eastern Mediterranean. *Marine Geol.* **11**, 261.

Venkatarathnam, K., Biscaye, P. E. and Ryan, W. B. F., 1971. Origin and dispersal of Holocene sediments in the eastern Mediterranean. **In** *Sedimentation in the Mediterranean Sea.* D. J. Stanley (Editor). Smithsonian Press. Washington, D.C.

Watson, J. A. and Johnson, G. L., 1969. The marine geophysical survey in the Mediterranean. *Int. Hydrog. Rev.* **46**, 81.

Wong, H. K. and Zarudzki, E. F. K., 1969. Thickness of unconsolidated sediments in the eastern Mediterranean Sea. *Bull. Geol. Soc. Am.* **80**, 1611.

Wong, H. K., Zarudzki, E. F. K., Phillips, J. D. and Giermann, G. K. F., 1971. Some geophysical profiles in the eastern Mediterranean. *Bull. Geol. Soc. Am.* **82**, 91.

Woodside, J. M. and Bowin, C. O., 1970. Gravity anomalies and inferred crustal structure in the eastern Mediterranean Sea. *Bull. Geol. Soc. Amer.* **81**, 1107.

Site Summary 130

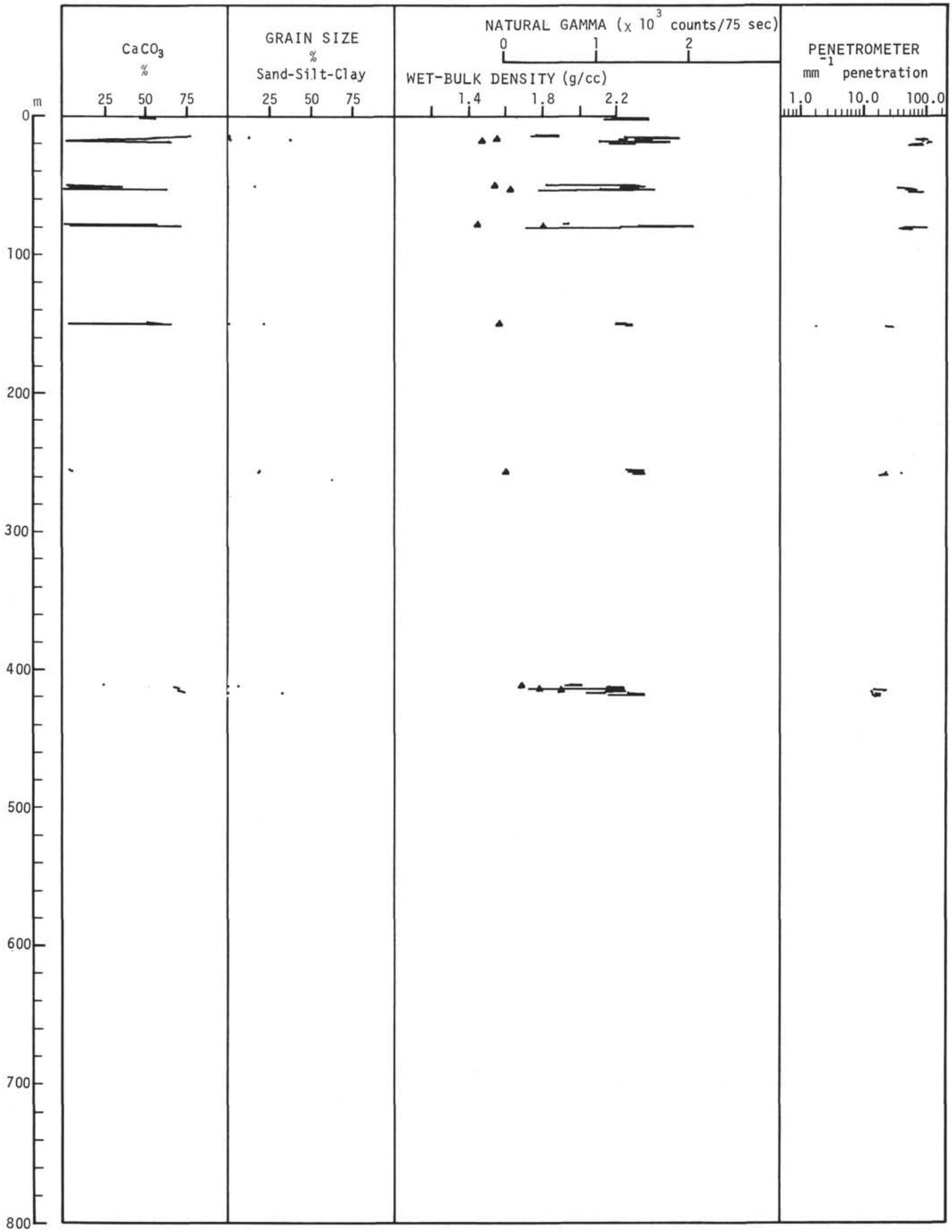

AGE	LITHOLOGY AND BIOSTRATIGRAPHY	LITHOLOGY

PLEISTOCENE — abundant displaced (?) PLIOCENE in Core 6

<u>Foraminiferal MARLS</u> (pelagics)

Light colored: light to olive gray, bedded, mottled, scattered forams, H_2S Odor, high $CaCO_3$ content = 40 to 70%

Sapropel bed at 14.1 m, ash layer in core 1-A.

foraminiferal assemblages indicate climatic fluctuations

14.5m

below 14.5m: <u>interbedded CLAYS and foraminiferal MARLS</u>

CLAYS: Nile influxes (turbidites)

beds of black clay with occasional coarse, silty or sandy base

sharp contacts between beds

low $CaCO_3$ content: 2 to 5%

H_2S odor

pyrite

burrow mottling in the upper part of the dark clay at contact with the overlying foraminiferal marls

displaced shallow-water benthonic faunas

Foraminiferal MARLS (pelagics)

light colored: light bluish gray

high $CaCO_3$ content: 40 to 70%

mottled

eroded top

foraminiferal assemblage indicate climatic fluctuations

displaced shallow-water benthonic fauna

components include siliceous sponge spicules and radiolaria

reworking of Cretaceous planktonic foraminifera suggests possible transition to Pliocene in cores 6 and 7, or alternatively allocthonous units of Pliocene sediments retransported into Pleistocene levels.

MARLS (redeposited pelagics)

beds of foraminiferal sand grading to marl ooze

erosional base

SAPROPELS

beds of black marl ooze, bready texture, sharp contacts, high pyrite content, in the *G. oceanica* zone.

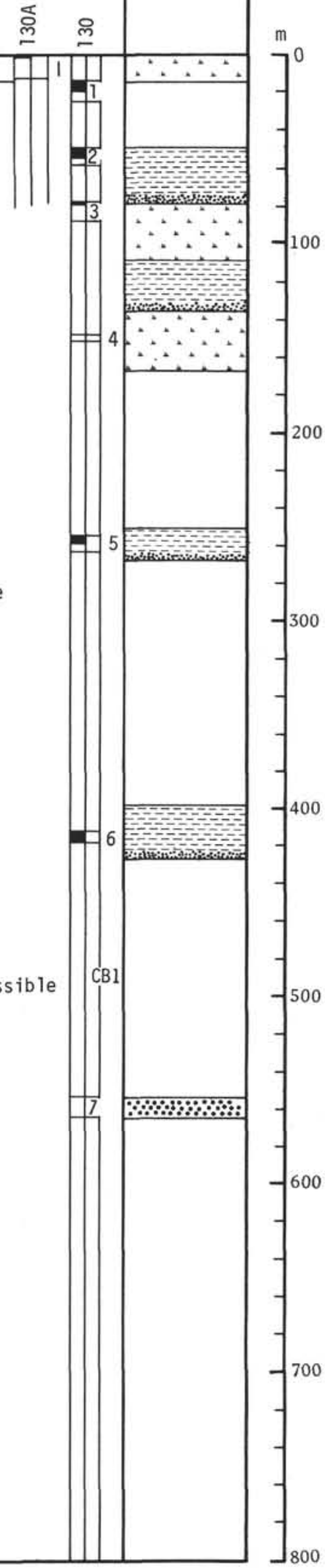

SITE 130 CORE 1 Cored Interval 13-23 m

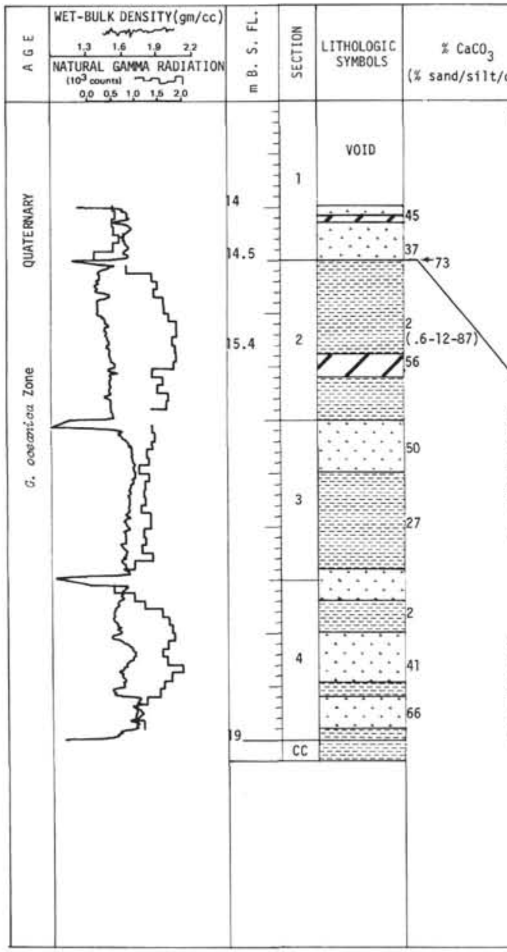

LITHOLOGY AND PALEONTOLOGY

DISTURBANCE: V, D, D

14-14.5 - FORAMINIFERAL MARLS (pelagics)

light colored: light gray (N7) to olive gray (5Y 5/1)
plastic, visible forams
bedded, microtectonic deformations in section 4
mottled
H_2S odor (122-135 cm, section 1)
sapropel bed, black, at 14.1 m

Smear

nannos	60
forams	5
calcite	10
quartz	5
mica	15
pyrite	5

below 14.5

CLAYS interbedded with FORAMINIFERAL MARLS

Clays (Nile influxes: turbidites)

black (N1)
plastic
H_2S odor
pyritic

Smear

nannos	10
clays	80
mica	
quartz, etc.	5

Foraminiferal marls (pelagics)

petrography as in section 1

Sapropel bed at 15.4

black (N1)
bready texture
sharp contacts

planktonic foraminifera abundant and diversified, indicating normal pelagic sedimentation in the intervals investigated (see range chart); no indications of cold intervals (pre-glacial Pleistocene?) pteropods, otoliths, organic matter are present discontinuously, but never abundant. rich nannofossil assemblage of the *Gephyrocapsa oceanica* zone, with some (little) reworking of Pliocene discoasters

SITE 130 CORE 2 Cored Interval 49-58 m

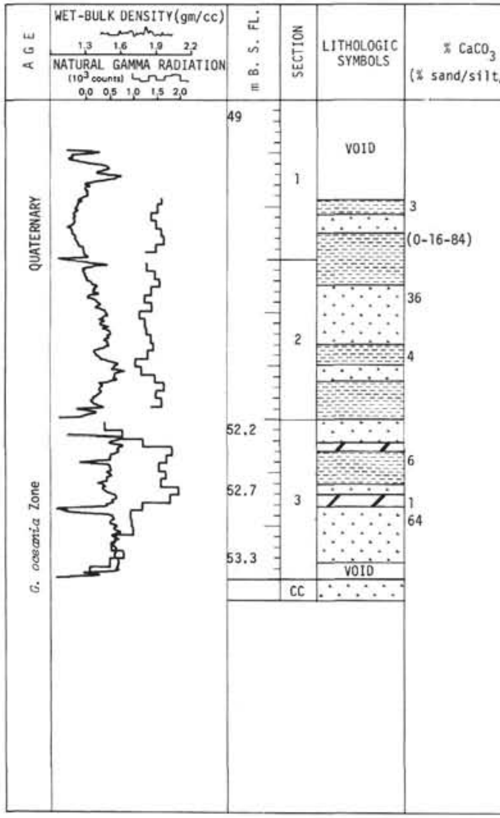

LITHOLOGY AND PALEONTOLOGY

DISTURBANCE: V, V

interbedded CLAYS and foram-MARL OOZES

clays (Nile influxes: turbidites)

very dark gray (N3)
plastic
low $CaCO_3$
occasional sand laminae at bottom
sharp contacts

Smear

nannos	10
mica	5
clay	70
pyrite	15

foram-marl oozes (pelagics)

light bluish gray (5B 7/1)
plastic
high $CaCO_3$
mottled
erosional contact on top

Smear

nannos	75
forams	10
quartz	5
mica	5
pyrite	5

2 sapropel beds at 52.2 and 52.7

black (N#0)
sharp contacts
bready texture

planktonic foraminifera abundant, indicating normal pelagic sedimentation. no indications of cold intervals (pre-glacial Pleistocene?) nannofossils of the *Gephyrocapsa oceanica* zone, also including some reworked Discoasters from the Pliocene and Eocene

SITE 130 CORE 3 Cored Interval 77-86 m

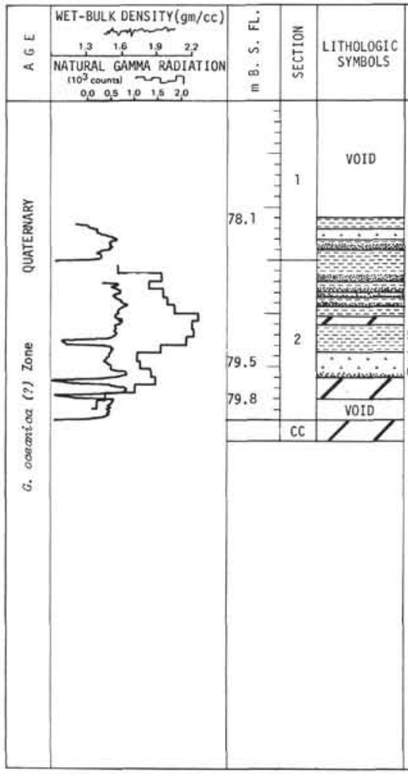

% $CaCO_3$ (% sand/silt/clay) | LITHOLOGY AND PALEONTOLOGY | DISTURBANCE

1
57
5
72
67

interbedded graded CLAYS, MARL OOZES and SAPROPELS

Clays (Nile influxes: turbidites)

sequences of dark gray (N3-N4) clay grading upward in lighter clay

sequences 10-30 cm thick

sharp contacts with quartzose sand laminae at the base and burrowing at top

low $CaCO_3$: 2-5%

Marl Oozes (redeposited pelagics)

three beds of homogeneous, olive gray (5Y 5/1) marl ooze, sharp contacts, high $CaCO_3$: 60-72%, no visible forams

one bed of foraminiferal sand grading in marl ooze at 79.5 m, sharp contacts and erosional base

Composite beds

four redeposited beds of mixed Nile clays and pelagics (section 2: 20-50 cm)

Sapropels

two layers, 5 and 20 cm thick, black (N#0), "bready" texture

planktonic foraminifera rare (Section 1, core catcher) or fairly abundant (Section 2, 23-25 cm) same interval also yields abundant pteropods; organic matter, ostracods, radiolarians, holothurian sclerites and hystricosphaerids are recorded in Section 1.
nannofossil assemblage with *Gephyrocapsa oceanica*, also yielding large specimens of *Braarudosphaera bigelowi*
nannofossils reworked from the Miocene and Pliocene.

SITE 130 CORE 4 Cored Interval 148-150 m

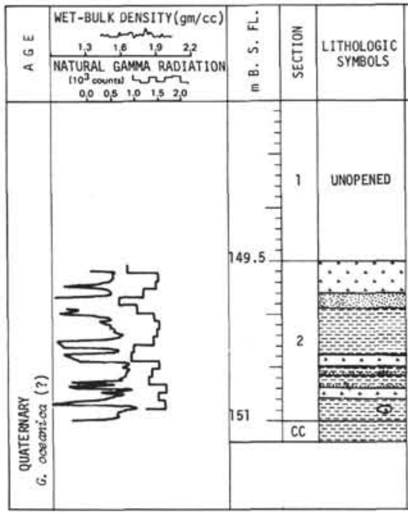

% $CaCO_3$ (% sand/silt/clay) | LITHOLOGY AND PALEONTOLOGY | DISTURBANCE

(1-19-80)
60
4
66

graded SANDS and CLAYS interbedded w/MARL OOZES

Sand-clay beds (Nile influxes: turbidites)

sequences 10-40 cm thick
quartzose sands w/sharp bottom contacts, grading to plastic, medium dark gray (N3) clay
low $CaCO_3$: 1-4%

Smear (sands)

quartz	75	apatite	3
hornblende	10	chlorite	2
pyrite	5	forams	2
plagioclase	3		

Marl Oozes (Pelagics)

light gray (N7) beds, 5-25 cm thick
visible forams
semi-indurated
high $CaCO_3$: 60-66%

rich planktonic foraminiferal assemblage in Section 2, including over 20 discrete taxa; abundant and diversified nannofossils, with *Gephyrocapsa oceanica* and *Pseudoemiliania lacunosa*; plenty of diatoms and sponge spicules in the core catcher

SITE 130 CORE 5 Cored Interval 254-263 m

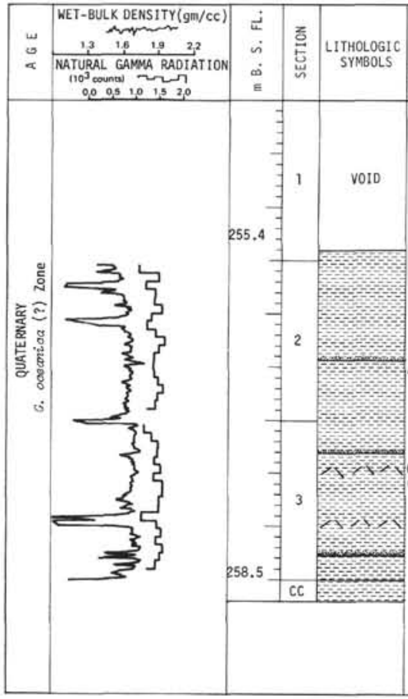

% $CaCO_3$ (% sand/silt/clay) | LITHOLOGY AND PALEONTOLOGY | DISTURBANCE

(0-20-80)
4
6
(0-19-81)

CLAY w/SAND laminae (Nile influxes: turbidites)

Clays

dark green (N3)
homogeneous
plastic to stiff
shaly

Smear

nannos	5
clays	80
pyrite	10
quartz	5

Sand Laminae

thin layers of quartzose sand occasionally lithified (in section 3)

Smear

quartz	30
mica	7
pyrite	55
hornblende	
plagioclase	
apatite	

planktonic foraminifera very rare, except in the core catcher where they are common and include some 15 species; organic matter and pyrite locally abundant; benthonic foraminifera absent in section 2; represented by deep-living forms in the core catcher
poor nannofossil assemblage

SITE 130 CORE 6 Cored Interval 411-418 m

AGE	WET-BULK DENSITY (gm/cc) 1.3 1.6 1.9 2.2 / NATURAL GAMMA RADIATION (10^3 counts) 0.0 0.5 1.0 1.5 2.0	m B. S. FL.	SECTION	LITHOLOGIC SYMBOLS	% $CaCO_3$ (% sand/silt/clay)	LITHOLOGY AND PALEONTOLOGY	DISTURBANCE
QUATERNARY *G. oceanica* (?) Zone	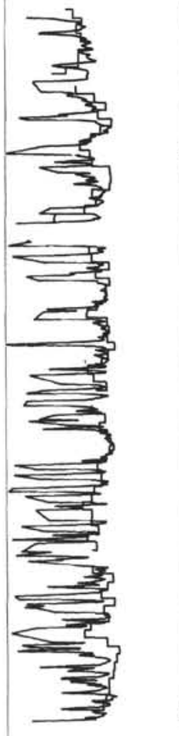	411.7	1	VOID	25 (0-6-94)	411.7-413.2 graded SANDS and CLAYS (Nile influxes: turbidites) sequences of sands grading to silts and clay. Sands: laminae to 3 cm thick; graded; oblique bedding; sharp bottom contact. Smear: quartz 40, pyrite 30, dolomite 5, calcite 10, hornblende 4	V
		413.2	2	VOID, sharp	68	Clays: dark gray (N3); indurated; shaly; low $CaCO_3$: 25%; moderate mottling	V
			3	VOID	71	413.2-418 MARL OOZE (pelagics): greenish gray (5GY 6/1); homogeneous; stiff; slightly shaly	V
			4	VOID	70	Smear: nannos 65, forams 5, mica 20, quartz 10, pyrite, etc.	V
			5	VOID	74 (0-33-67)	rich planktonic foraminiferal assemblage in Section 2; foraminifera scattered or rare in sections 3-5, where the sedimentation is terrigenous. Benthonic foraminifera fairly abundant in the core catcher, also including Miliolidae and *Discorbis*; calcareous nannofossils are abundant throughout the core and include rather abundant *Discoaster brouweri* (reworked?). Micrascidites of Tunicates	V
		418.5	CC				

SITE 130 CORE 7 Cored Interval 554-563 m

AGE	WET-BULK DENSITY (gm/cc) 1.3 1.6 1.9 2.2 / NATURAL GAMMA RADIATION (10^3 counts) 0.0 0.5 1.0 1.5 2.0	m B. S. FL.	SECTION	LITHOLOGIC SYMBOLS	% $CaCO_3$ (% sand/silt/clay)	LITHOLOGY AND PALEONTOLOGY	DISTURBANCE
QUATERNARY *P. lacunosa* Zone		554	CC			Lithic SANDSTONE: two pieces 10, and 7.5 cm long; medium dark gray (N4); embedded pebbles of consolidated ooze, 1-10 cm across, greenish gray w/mottles. Thin section (sandstone): quartz 80, plagioclase 5, hornblende 5, pyrite 5, apatite, mica, forams. X-rays: quartz, calcite, feldspar. poor nannofossil assemblage containing *Braarudosphaera bigelowi*; poor foraminiferal assemblage. Total Drilling: 563 m in sandstone	

SITE 130A CORE 1A Cored Interval 0-11 m

AGE	WET-BULK DENSITY (gm/cc) 1.3 1.6 1.9 2.2 / NATURAL GAMMA RADIATION (10^3 counts) 0.0 0.5 1.0 1.5 2.0	m B. S. FL.	SECTION	LITHOLOGIC SYMBOLS	% $CaCO_3$ (% sand/silt/clay)	LITHOLOGY AND PALEONTOLOGY	DISTURBANCE
		0	1	AAAAA	47, 57	MARL OOZE (pelagics): beds, 2-30 cm thick, separated by sharp contacts, yellowish brown (10YR 5/6) to light gray (N7); ash layer at 0.35 m; sapropel: black (N#1) layer at the base. Smear (marl ooze): nannos 55, forams 2, mica 28, quartz 15, pyrite. Ash: glass 40, nannos 50, mica 10, pyrite. entire climatic cycle is represented in Section 1, with the coldest interval present at 14-16 cm. (see report on biostratigraphy) nannofossils belonging to the *Emiliania huxleyi* zone	
		1.5	CC				

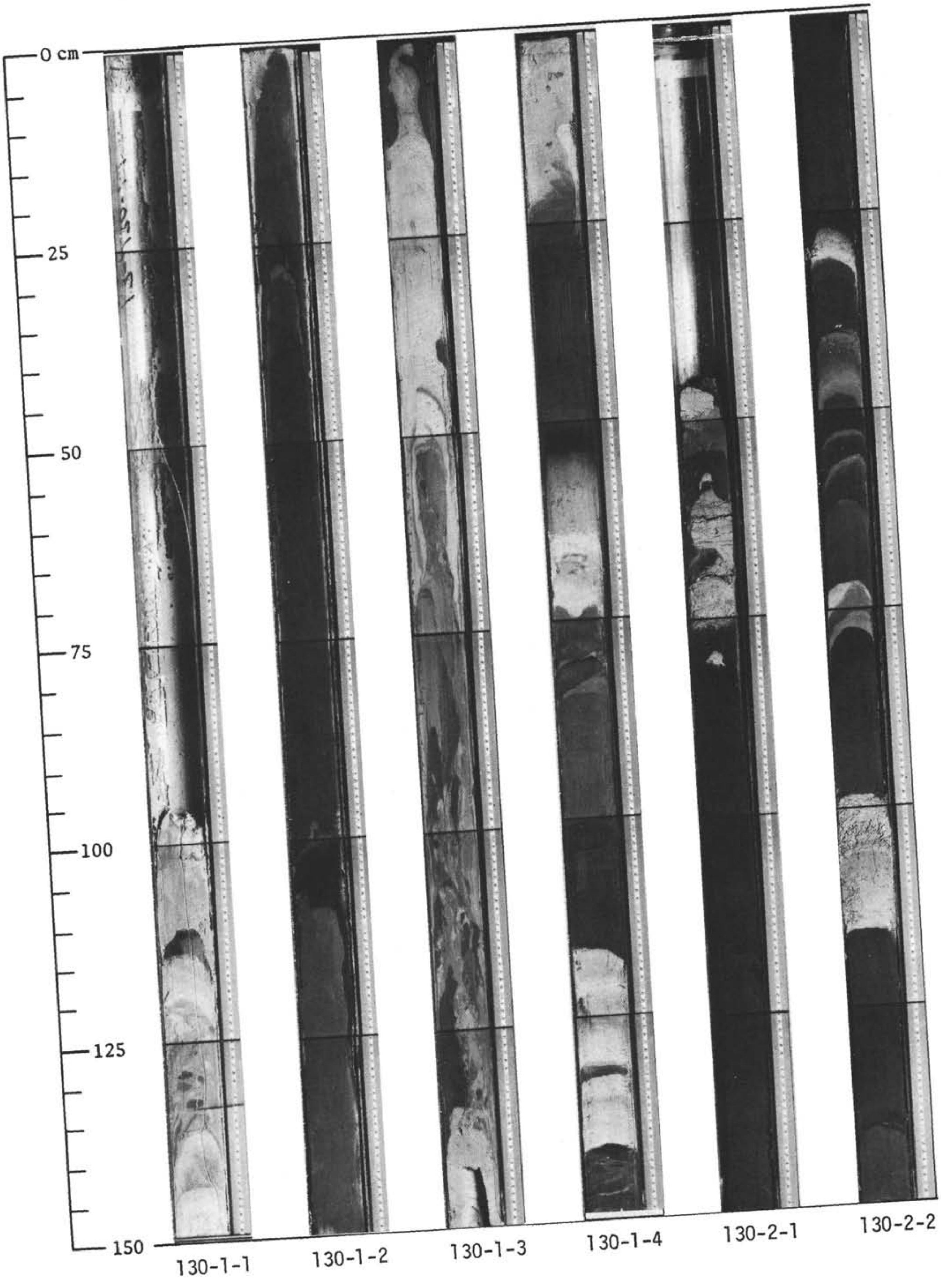
0 cm
25
50
75
100
125
150
130-1-1
130-1-2
130-1-3
130-1-4
130-2-1
130-2-2

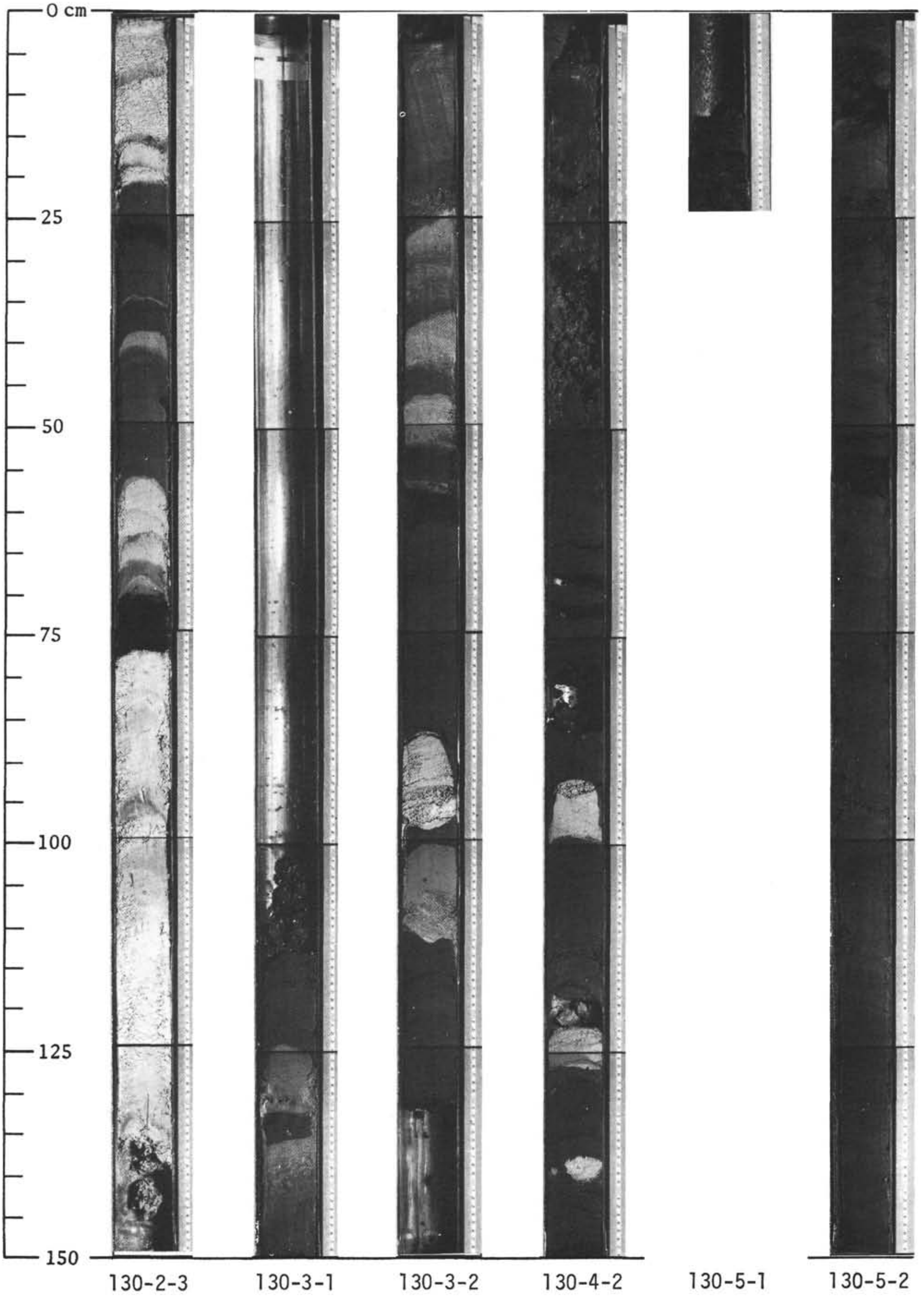
0 cm
25
50
75
100
125
150
130-2-3
130-3-1
130-3-2
130-4-2
130-5-1
130-5-2

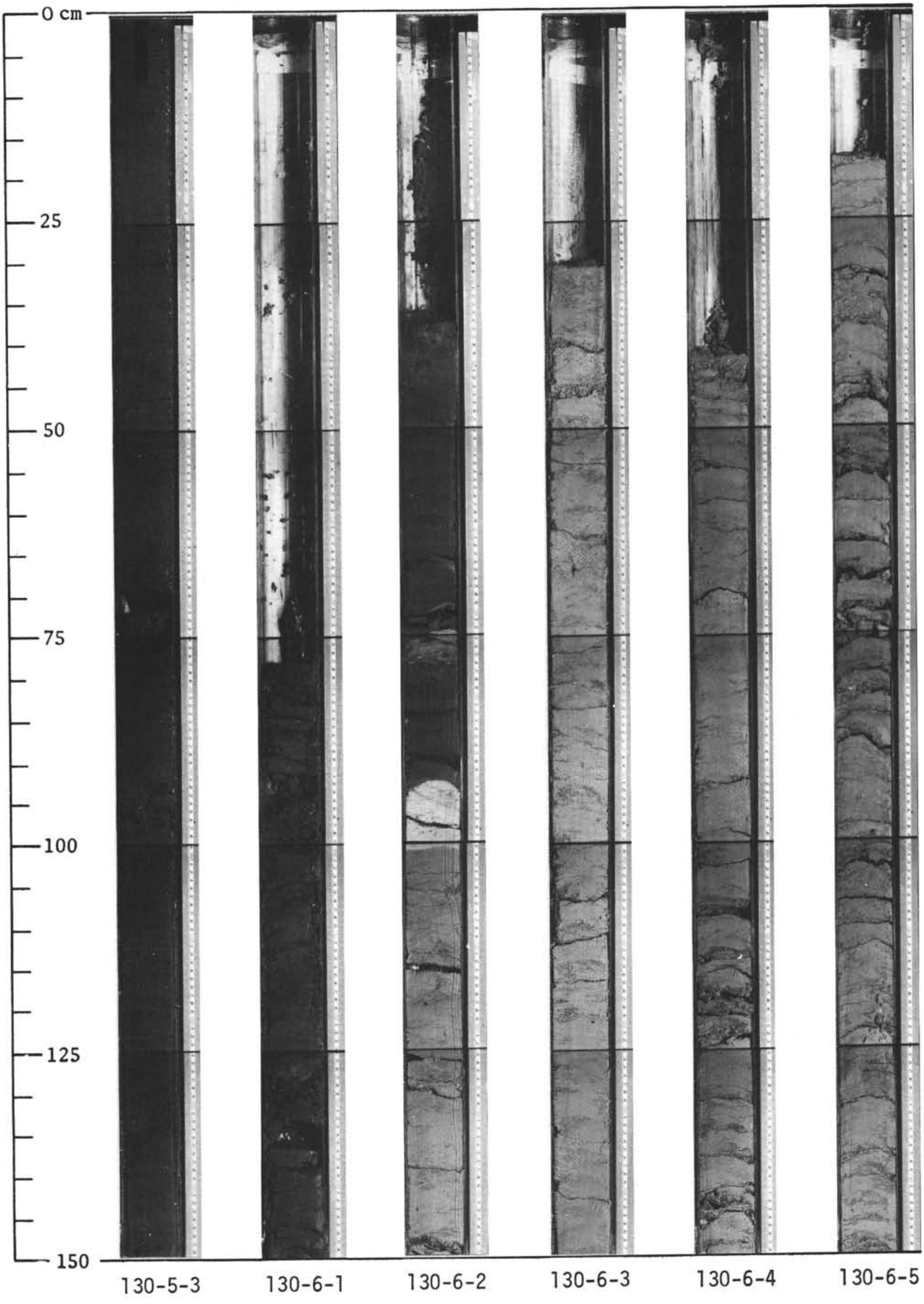
0 cm
25
50
75
100
125
150
130-5-3
130-6-1
130-6-2
130-6-3
130-6-4
130-6-5

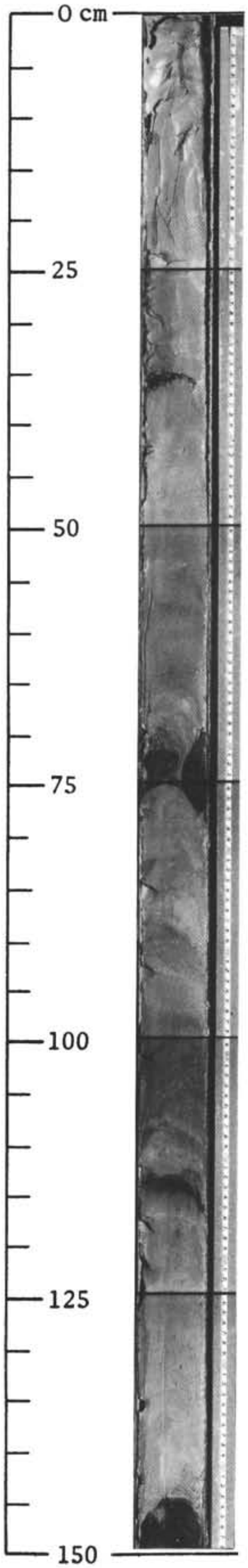

130A-1-1